

An-Najah National University

Faculty of Graduate studies

**Nanocrystalline Cellulose Modified with
Aromatic Amine Cleating Agent:
Synthesis and Evaluation as an
Adsorbent for Toxic Metal Ions**

By

Majdi Nedal Mohammad Qaisy

Supervisor

Prof. Othman Hamed

Co-Supervisor

Dr. Ibrahim Abu Shqair

**This is Thesis Submitted in Partial Fulfillment of the Requirements
for the Degree of Master of Chemistry, Faculty of Graduate Studies, An-
Najah National University, Nablus, Palestine.**

2021

**Nanocrystalline Cellulose Modified with Aromatic
Amine Cleating Agent: Synthesis and Evaluation as an
Adsorbent for Toxic Metal Ions**

By

Majdi Nedal Mohammad Qaisy

This Thesis was defended successfully on 4 / 4 /2021 and approved by:

Defense Committee Members

Signature

– Prof. Othman Hamed / Supervisor

..........

– Dr. Ibrahim Abu Shqair / Co-Supervisor

..........

– Dr. Addalhadi Daghlas / External Examiner

..........

– Dr. Nidal Zatar / Internal Examiner

..........

III

Dedication

I dedicate my thesis to God Almighty my creator, my strong pillar, my source of inspiration, wisdom, knowledge, and understanding.

I also dedicate this thesis to my beloved grandmother. To whom I Prefer about myself, (my mother). To my father, God gives him long life and to my all sisters and brothers.

I dedicate this work also to my teachers who were not stingy with their knowledge and effort throughout the foundation stage in the school, and to my creative and distinguished doctors and professors who had a great role in my personal development and my thinking in many aspects, whether in the cognitive or moral side.

To everyone who lights the way of others by his knowledge.

Acknowledgment

Foremost, I would like to express my sincere gratitude to my advisor Prof. Othman Hamed. His kindly oversight of this thesis constantly gave me the motivation to perform to my maximum ability. I was very fortunate to have been able to work with him.

I must also thank Dr. Ibrahim Abu Shqair, for his help and precious advice. His detailed and constructive comments were vital to the development of this thesis.

I dedicate a corner decorated with roses and scented with musk to thank my professor Prof. Hikmat Hilal, who I always felt the sophistication of his knowledge, the splendor of his courses and his teaching strategy.

I also extend my thanks and gratitude to my teachers in the various stages of my education from foundation to this day, and I thank my colleagues who accompanied me in this stage and who I am proud of their friendship and good companionship for the knowledge and moral support they provided me in its various forms. In particular, Mr. Qais Wawi, Mrs. Rafif Adwan and Mr. Abed Daraghme.

I would like to thank the rest of my thesis committee for their encouragement, insightful comments, and questions.

My family members, I'm extremely grateful for your love, prayers, caring and tremendous encouragement, and support.

الإقرار

أنا الموقع أدناه مقدم الرسالة التي تحمل العنوان:

Nanocrystalline Cellulose Modified with Aromatic Amine Cleating Agent: Synthesis and Evaluation as an Adsorbent for Toxic Metal Ions

أقر بأن ما اشتملت عليه هذه الرسالة إنما هي من نتاج جهدي الخاص، باستثناء ما تمت الإشارة ليه
حيثما ورد، وأن هذه الرسالة ككل أو أي جزء منها لم يقدم من قبل لنيل أي درجة علمية أو بحث
علمي أو بحثي لدى أي مؤسسة تعليمية أو بحثية أخرى

Declaration

The work provided in this thesis, unless otherwise referenced, is the researcher's own work, and has not been submitted elsewhere for any other degree or qualification.

Student's Name:

اسم الطالب: مجدي نضال محمد قيسي

Signature:

التوقيع: 

Date:

التاريخ: 4/4/2021

Table of contents

No.	Content	Page
	Dedication	III
	Acknowledgement	IV
	Declaration	V
	Table of contents	VI
	List of tables	IX
	List of Schemes	XI
	List of figures	XII
	List of abbreviations	XIV
	Abstract	XVII
I	Chapter One: Introduction	1
1.1	Water Pollution	2
1.2	Heavy Metals	4
1.2.1	Copper	5
1.2.2	Lead	6
1.3	The Concept of Water Purification	7
1.3.1	Adsorption	9
1.3.2	Classification of Adsorbents	10
1.4	Cellulose	12
1.4.1	Cellulose Structure	14
1.4.2	Related Research	14
1.4.3	Nanocrystalline Cellulose (NCC)	16
1.4.4	1-Phenylbiguanide (PBG)	18
II	Chapter Two: Experimental	20
2.1	Instrumentation	20
2.2	Materials	20
2.3	Methods	21
2.3.1	Converting Cellulose to Nanocrystalline Cellulose (NCC)	21
2.3.2	Oxidation of Nanocrystalline Cellulose (NCC)	22
2.3.2.1	Extent of Oxidation	23
2.3.2.2	Derivatization of Cellulose Dialdehyde	24
2.3.2.3	Reduction of NCC-PBG-A	24
2.4	Preparation of Standard Solutions	25
2.5	Calibration Curves	25
2.6	Batch Experiments	27
2.6.1	Effect of Adsorbent Weight (Dosage)	27
2.6.2	Effect of Adsorbate Concentration	28
2.6.3	Effect of Time	29

VII

2.6.4	Effect of pH Value	31
2.6.5	Effect of Temperature	32
2.7	Adsorption Kinetics	33
2.8	Adsorption Thermodynamics	34
2.9	Wastewater Purification	37
III	Chapter Three: Results and Discussion	38
3.1	Oxidation of NCC to 2,3- Dialdehyde Cellulose	38
3.1.1	Determination of Aldehyde Content	39
3.1.2	Detection of Aldehyde by FT-IR	40
3.2	Cross-linking the Dialdehyde with Phenylbiguanide	41
3.2.1	Detection of Imine in Polymer(NCC-PBG-A) by FT-IR	42
3.2.2	Conversion of Imine into an Amine by Reduction	43
3.2.3	FT-IR for Polymer (NCC-PBG-B)	44
3.4	Adsorption Results	45
3.4.1	Adsorption of Copper Ions (Cu^{2+})	46
3.4.1.1	Effect of Contact Time	46
3.4.1.2	Effect of pH Value	47
3.4.1.3	Effect of Temperature	49
3.4.1.4	Effect of Adsorbent Dosage	50
3.4.1.5	Effect of Copper Ions (Cu^{2+}) Ion Concentration	51
3.4.2	Adsorption of Lead Ions (Pb^{2+})	54
3.4.2.1	Effect of Contact Time	54
3.4.2.2	Effect of pH Value	55
3.4.2.3	Effect of Temperature	57
3.4.2.4	Effect of Adsorbent Dosage	58
3.4.2.5	Effect of Pb^{2+} Initial Concentration	60
3.5	Adsorption Kinetics	62
3.5.1	Adsorption of Cu^{2+} Ions	63
3.5.1.1	Testing the Two Models on NCC-PBG-A	63
3.5.1.2	Testing the Two Models on NCC-PBG-B	65
3.5.2	Adsorption of Pb^{2+} Ions	67
3.5.2.1	Testing the Two Models on NCC-PBG-A	67
3.5.2.2	Testing the Two Models on NCC-PBG-B	69
3.6	Adsorption Isotherms	72
3.6.1	Adsorption of Cu^{2+}	74
3.6.1.1	Testing the Two Models on NCC-PBG-A	74
3.6.1.2	Testing the Two Models on NCC-PBG-B	76
3.6.2	Adsorption of Pb^{2+}	78
3.6.2.1	Testing the Two Models on NCC-PBG-A	78
3.6.2.2	Testing the Two Models on NCC-PBG-B	80
3.7	Adsorption Thermodynamics	83

VIII

3.7.1	Adsorption of Cu^{2+}	83
3.7.1.1	Testing the Thermodynamic Equation on NCC-PBG-A	83
3.7.1.2	Testing the Thermodynamic Equation on NCC-PBG-B	85
3.7.2	Adsorption of Pb^{2+}	86
3.7.2.1	Testing the Thermodynamic Equation on NCC-PBG-A	86
3.7.2.2	Testing the Thermodynamic Equation on NCC-PBG-B	87
3.8	Analysis for Samples of Sewage Before & After the Purification Process	89
3.9	Conclusion	91
	Recommendations	92
	References	93
	الملخص	102

List of Tables

No.	Table	Page
2.1	Effect of the Wt. of dosage of NCC-PBG-(A & B) for the adsorption of both Cu^{2+} and Pb^{2+} ions	28
2.2	Effect of the Conc. of adsorbate on the adsorption of both Cu^{2+} and Pb^{2+} ions on the NCC-PBG-(A & B)	29
2.3	Effect of the shaking time on the adsorption of both Cu^{2+} and Pb^{2+} ions on the NCC-PBG-(A & B)	30
2.4	Effect of the pH value on the adsorption of both Cu^{2+} and Pb^{2+} ions on NCC-PBG-(A & B)	31
2.5	Effect of the temperature on the adsorption of both Cu^{2+} and Pb^{2+} ions on NCC-PBG-(A & B)	32
3.1	The adsorption results for Cu^{2+} ions using NCC-PBP-(A & B)	53
3.2	The adsorption results for removing Pb^{2+} from soln. using NCC-PBP-(A & B)	61
3.3	Pseudo-first order model for the adsorption of Cu^{2+} on NCC-PBG-A	63
3.4	Pseudo-second order model for the adsorption of Cu^{2+} on NCC-PBG-A	64
3.5	Pseudo-first order model for the adsorption of Cu^{2+} on NCC-PBG-B	65
3.6	Pseudo-second order model for the adsorption of Cu^{2+} on NCC-PBG-B	66
3.7	Pseudo-first order model for the adsorption of Pb^{2+} on NCC-PBG-A	67
3.8	Pseudo-second order model for the adsorption of Pb^{2+} on NCC-PBG-A	68
3.9	Pseudo-first order model for the adsorption of Pb^{2+} on NCC-PBG-B	69
3.10	Pseudo-second order model for the adsorption of Pb^{2+} on NCC-PBG-B	70
3.11	Summary of adsorption kinetic	71
3.12	Langmuir model for adsorption of Cu^{2+} on NCC-PBG-A	74
3.13	Freundlich model for adsorption of Cu^{2+} on NCC-PBG-A	75
3.14	Langmuir model for adsorption of Cu^{2+} on NCC-PBG-B	76
3.15	Freundlich model for adsorption of Cu^{2+} on NCC-PBG-B	77

3.16	Langmuir model for adsorption of Pb^{2+} on NCC-PBG-A	78
3.17	Freundlich model for adsorption of Pb^{2+} on NCC-PBG-A	79
3.18	Langmuir model for adsorption of Pb^{2+} on NCC-PBG-B	80
3.19	Freundlich model for adsorption of Pb^{2+} on NCC-PBG-B	81
3.20	Summary Adsorption Isotherms for NCC-PBG-(A & B)	82
3.21	Thermodynamic results for adsorption of Cu^{2+} on NCC-PBG-A	83
3.22	Thermodynamic results for adsorption of Cu^{2+} on NCC-PBG-B	85
3.23	The thermodynamic parameters for the adsorption of Cu^{2+} on NCC-PBG-(A & B)	86
3.24	Thermodynamic results for adsorption of Pb^{2+} on NCC-PBG-A	86
3.25	Thermodynamic results for adsorption of Pb^{2+} on NCC-PBG-B	87
3.26	The thermodynamic parameters for the adsorption of Pb^{2+} on NCC-PBG-(A & B).	88
3.27	Results of the center of analyzes for the Conc. of toxic metals	90

List of Scheme

No.	Scheme	Page
3.1	Conversion of NCC to cellulose dialdehyde.	38
3.2	Mechanism for oxidation of NCC	39
3.3	Crosslinked the NCC (Dialdehyde) with PBG	41
3.4	Preparation of the NCC-PBG-B polymer from NCC-PBG-A polymer	43

List of Figures

No.	Figure	Page
1.1	Cellulose structure	14
1.2	Phenyl biguanide structure	18
2.1	Calibration curve of lead Pb^{2+} .	26
2.2	Calibration curve of copper Cu^{2+} .	26
3.1	FT-IR spectra of oxidized cellulose (Dialdehyde NCC)	40
3.2	FT-IR spectra of polymer NCC-PBG-A	42
3.3	FT-IR spectra of polymer NCC-PBG-B	44
3.4	Effect of contact time on the adsorption of Cu^{2+} on NCC-PBG-(A & B)	46
3.5	Effect of pH value on the adsorption of Cu^{2+} on NCC-PBG-(A & B)	48
3.6	Effect of temperature on the adsorption of Cu^{2+} on NCC-PBG-(A & B)	49
3.7	Effect of adsorbent dosage on the adsorption of Cu^{2+} on NCC-PBG-(A & B)	50
3.8	Effect of adsorbate Conc. on the adsorption of Cu^{2+} on NCC-PBG-(A & B)	52
3.9	Effect of contact time on the adsorption of Pb^{2+} ions on NCC-PBG-(A&B)	54
3.10	Effect of pH value on the adsorption of Pb^{2+} on NCC-PBG-(A&B)	56
3.11	Effect of temperature on the adsorption of Pb^{2+} on NCC-PBG-(A&B)	57
3.12	Effect of adsorbent dosage on the adsorption of Pb^{2+} on NCC-PBG-(A&B)	58
3.13	Effect of adsorbent dosage on the adsorption of Pb^{2+} on NCC-PBG-(A&B)	60
3.14	Pseudo-first order model for the adsorption of Cu^{2+} on NCC-PBG-A	63
3.15	Pseudo-second order model for the adsorption of Cu^{2+} on NCC-PBG-A	64
3.16	Pseudo-first order model for the adsorption of Cu^{2+} on NCC-PBG-B	65
3.17	Pseudo-second order model for the adsorption of Cu^{2+} on NCC-PBG-B	66
3.18	Pseudo-first order model for the adsorption of Pb^{2+} on NCC-PBG-A	67

XIII

3.19	Pseudo-second order model for the adsorption of Pb ²⁺ on NCC-PBG-A	68
3.20	Pseudo-first order model for the adsorption of Pb ²⁺ on NCC-PBG-B	69
3.21	Pseudo-second order model for the adsorption of Pb ²⁺ on NCC-PBG-B	70
3.22	Langmuir model for adsorption of Cu ²⁺ on NCC-PBG-A	74
3.23	Freundlich model for adsorption of Cu ²⁺ on NCC-PBG-A	75
3.24	Langmuir model for adsorption of Cu ²⁺ on NCC-PBG-B	76
3.25	Freundlich model for adsorption of Cu ²⁺ on NCC-PBG-B	77
3.26	Langmuir model for adsorption of Pb ²⁺ on NCC-PBG-A	78
3.27	Freundlich model for adsorption of Pb ²⁺ on NCC-PBG-A	79
3.28	Langmuir model for adsorption of Pb ²⁺ on NCC-PBG-B	80
3.29	Freundlich model for adsorption of Pb ²⁺ on NCC-PBG-B	81
3.30	Van't Hoff plot for the adsorption of Cu ²⁺ on NCC-PBG-A	84
3.31	Van't Hoff plot for the adsorption of Cu ²⁺ on NCC-PBG-B	85
3.32	Van't Hoff plot for the adsorption of Pb ²⁺ on NCC-PBG-	86
3.33	Van't Hoff plot for the adsorption of Pb ²⁺ on NCC-PBG-B	87

List of Abbreviations

Symbol	Abbreviation
PBG	Phenyl biguanide
FT-IR	Fourier Transform Infrared
OISW	Olive Industry Solid Wastes
BOD	Biological Oxygen Demand
COD	Chemical Oxygen Demand
EPA	Environmental Protection Agency
WHO	World Health Organization
ΔE	Activation Energy
HBB	Haemoglobin Beta
R^2	Correlation coefficient (regression coefficient, fitting coefficient)
NCC	Nanocrystalline Cellulose
3D	Three Dimensional
ICP-MS	Inductively Coupled Plasma Mass Spectrometry
ICE	Immigration and Customs Enforcement's
FAAS	Flame Atomic Adsorption Spectrometer
Ads.	Adsorption
Soln.	Solution
Eq.	Equation
NCC-PBG-A	cross-linked poly(acrylic acid)grafted with lignin polymer A
NCC-PBG-B	cross-linked poly(acrylic acid)grafted with lignin polymer B
OC	Oxidized Cellulose
Ald	Aldehyde
Conc.	Concentration
Fig.	Figure
W	Weight
Temp.	The temperature ($^{\circ}\text{C}$)
C_e	Concentration of metal ions in the sample solution after treatment at equilibrium (mg/L)
C_i	Initial concentration of metal ions in the sample solution (mg/L)
q_e	The mass of adsorbate adsorbed per unit mass of adsorbent at equilibrium (mg/g)
q_t	Amount of adsorbate per unit mass of adsorbent at time t (min)

Q_{\max}	Maximum monolayer adsorption capacity of the adsorbent (mg/g) theoretically
K_1	The pseudofirst order rate constant
K_2	The pseudo second order rate constant
K_f	Freundlich constant which is an approximate indicator of adsorption capacity of the sorbent (mg/g (L/mg) ^{1/n})
K_L	Langmuir isotherm constant (L/mg)
K_d	The thermodynamic gas constant
$\frac{1}{n}$	Dimensionless Freundlich constant giving an indication of how favorable the adsorption process
R_L	Dimensionless constant separation factor
H	The change in enthalpy
S	The change in entropy
G	The change in Gibbs free energy
R	The universal gas constant
T	The absolute temperature

Nanocrystalline Cellulose Modified with Aromatic Amine Cleating Agent: Synthesis and Evaluation as an Adsorbent for Toxic Metal Ions

By

Majdi Nedal Mohammad Qaisy**Supervisor****Prof. Othman Hamed****Co-Supervisor****Dr. Ibrahim Abu Shqair****Abstract**

Recently, water polluted with heavy toxic elements is getting high attention from scientists all over the world. Many recent studies tend to develop appropriate methods for removing these substances, and it is important that these methods be low cost and environmentally friendly, so they will commercially and practically more attractive. In this study, the advantages of cellulose were exploited and harnessed in the purification of wastewater contaminated with heavy metal ions, where a three-dimensional branched and cross-linking polymer was prepared for use in the purification process.

In the beginning, the natural cellulose polymer extracted from the solid waste of the olive industry (OISW) was converted to nanocrystalline cellulose (NCC), and then oxidation of the nanocrystalline cellulose was carried out by using sodium periodate (NaIO_4) to produce a dialdehyde. Finally, the dialdehyde obtained from the previous step was converted into imine by reacting it with 1- phenyl biguanide, which then reduced to amine using the mild reducing agent sodium borohydride.

Two types of polymers were prepared: The first type was formed upon binding of 1-phenylbiguanide molecules to aldehyde groups in the oxidized

cellulose prepared in the previous step to form a modified cellulose polymer (NCC-PBG-A) that carries an imine functional group and also carries amine functional groups. A portion of the polymer containing the imine group produced in the final step was treated with sodium borohydride to prepare the type II polymer (NCC-PBG-B).

The prepared polymers were analyzed by FT-IR. The activity of the polymers and their adsorption ability for copper (Cu^{2+}) and lead (Pb^{2+}) ions were examined. Factors affecting the adsorption process such as mass of adsorbents, concentration of metal ions in the aqueous solution, temperature, pH and time were examined. The highest polymer efficiency was obtained (NCC-PBG-A) to remove copper ions at a concentration of 1.0 ppm copper ions, 100.0 mg of polymer, at room temperature of 25°C , pH is 7.0 upon stirring for 10.0 minutes. The same polymer also showed better absorption efficiency for lead ions (Pb^{2+}) at a concentration of 5.0 ppm lead ions, 100 mg of the polymer, at room temperature of 25.0°C , pH is 7.0 upon stirring for 10.0 minutes. As for the (NCC-PBG-B) polymer, the highest efficiency towards lead ions was shown at a concentration of 10.0 ppm lead ions, 50.0 mg of polymer, at 15.0°C , and a pH of 7.0 when stirred for 5.0 minutes. The same polymer also showed better absorption efficiency for lead ions (Pb^{2+}) at a concentration of 15.0 ppm lead ions, 50.0 mg of polymer, at 15.0°C , and pH 7.0 upon stirring for 10.0 minutes.

Thermodynamics and kinetic studies have shown that the removal of copper and lead ions using these polymers follow the second-order kinetics. The

XVIII

theoretical value of q_e (calc.) is close in magnitude to the experimental q_e (exp.). This indicates that the strong adsorption may be the rate determining step of adsorption process. The adsorption process is classified as exothermic and these results demonstrate that this work can be readily provided to make a highly effective adsorbent material.

CHAPTER ONE

INTRODUCTION

Preface

The world's population is increasing, and its various demands are increasing. To ensure the continuation of life, it is imperative to fulfill these demands, represented in many aspects, the first and most important of which are water and food. There are many sources that meet these needs, and here it must be pointed out that these sources have become significantly depleted due to the rapid growth in the population of the earth. This may make these sources unable to provide the necessities of life in the near future.

Water is one of the most important basic elements on which the planet Earth stands, as it constitutes 71.0% of the Earth's area. Many products depend on water to be prepared. Like paper and oil, just as water is used in the manufacture of many foodstuffs, and the great revolution in the exploitation of water resources is their use in generating electricity, which forms the basis of the industrial revolution in the generation of our world, as in our developed world.

Water is characterized by its ability to dissolve a lot of organic and inorganic materials. Which makes it important in many vital areas on one hand, and on the other hand, it is the reason that makes it easy to be contaminated with many materials that are difficult to separate and rotting water as a result of the activity of anaerobic bacteria, and this poses a threat to life of living organisms, especially humans [1].

Therefore, many scientific researches are directed towards wastewater recovery, integrated management, reclamation, reuse and recycling as tools for improving water resource management and most importantly motivating stakeholders and decision makers in this very important issue.

1.1 Water Pollution

At the global level, the problem of water quality is receiving great global attention, whether from industrially developed countries or even developing countries (third world countries), as water has been exposed to pollution in addition to great depletion as a result of the fierce and rapid growth in the population of the earth on which the increase in water demand is based [2]. Clean and different life requirements, the most important of which are industrial and food.

Sources of water pollution are classified into sources resulting from the waste of living organisms, including what is caused by many human activities, which is the most widespread, such as: sewage water, agricultural fertilizers, pesticides, food processing waste, and heavy metal ions such as copper, nickel, cadmium, cobalt and lead , Vanadium, cesium, zinc, and mercury, which are classified as chemical wastes resulting from industrial waste, and others [3].

In naturally occurring, organic matter is biodegraded by microbes and turns into substances that bring benefits to aquatic life. However, some chemical pollutants, such as the previously mentioned toxic heavy metals, are very harmful and toxic, even at concentrations of parts per billion (parts per

billion). There are some minerals beneficial to human and animal health and also for agriculture, such as zinc (Zn), copper (Cu), iron (Fe) and others within these types of beneficial minerals in very small doses and there are some compounds such as cyanide, thiocyanide, phenolic compounds, fluoride, radioactive materials, etc, which are considered dangerous to human, animal and plant life [4].

Removing toxic minerals from wastewater is one of the most difficult challenges in providing safe and potable water for all, as well as for protecting the environment. Where mineral contaminated water causes many diseases such as nervous system disorders, kidney disease, retardation, cancer and anemia [5]. Therefore, it is imperative to find ways to get rid of such pollutants and recycle water to achieve the greatest benefit from it and reduce the risk of its depletion.

1.2 Heavy Metals

Minerals are the most dangerous pollutant from the internationally classified pollutants, which are natural materials that have been removed from the ground and used in the manufacture of many human supplies for a long period of time. As minerals are characterized by their strong ability to bind to specific tissues in the human body; And their high potential to be toxic even when exposed in relatively small amounts [6].

Most of the surface and groundwater sources are contaminated with many heavy and toxic metals resulting from human activities or geological reasons. These mineral ions accumulate in the environment and nutrients. They enter the human body through the food chain and result in enlargement of the organs responsible for eliminating toxins from the body such as liver and kidneys [3].

Toxic heavy metals (Pt, Pd, Ag, Cu, Cd, Pb, Hg, Ni, Co, Zn and others) are naturally present in the earth's crust and these elements are present in the environment as a result of weather factors and rock erosion, including what is introduced into ecosystems from wastewater generated by human sources such as chemical manufacturing and mining, welding, alloying, paint, tanning, battery manufacture and the use of fertilizers and pesticides that carry this type of mineral [7].

The presence of such toxic ions in the water, even in low concentrations, resulted in the deterioration of water and drinking water resources. These ions are easily bound in the tissues of the human body, and this results in a variety of diseases and disorders [8]. Therefore, it is essential to purify industrial effluents from these toxic ions for their subsequent safe disposal. Numerous treatments have been studied to remove heavy metals from water, from expensive chemical treatment to low-cost natural adsorption methods [7]. However, the removal did not materialize as expected, and researchers are still developing more effective and less expensive filters.

We will now recognize some toxic heavy metals such as copper (Cu) and lead (Pb) to which water is exposed and threatens life on Earth, which we will conduct our study on in this work.

1.2.1 Copper

Our bodies need small doses of copper, so it is imperative that we get it in the food chain, because the body is unable to manufacture it, as most natural foods from animal sources contain copper. Among the most important sources rich in copper in large quantities are; liver and shellfish [9]. Copper is one of the essential trace elements, as it ranks third after iron and zinc in terms of trace elements in the bodies of living things.

Symptoms of gastrointestinal poisoning appear at concentrations of 3.0 ppm copper in the blood [10]. Therefore, chelating agents (CaNa₂EDTA, BAL) are recommended in this case [11].

1.2.2 Lead

Lead is a very toxic substance, as its presence in the body affects many organs and systems and specifically harms children. Lead gets distributed throughout the body to the brain, liver, kidneys and bones, and is stored in teeth and bones where it builds up over time [12]. Poisoning by it is a major and common threat to public health in developing countries that results from some human activities such as mining, agriculture and use leaded gasoline and paint. According the to Environmental Protection Agency (EPA),

exposure to lead causes various cancers, neurological and kidney damage, and impaired reproduction in both humans and animals [13].

It is known medically that the level of lead in the human body can be assessed by measuring the concentration of lead in his blood. There is no known concentration of lead that is safe and does not expose the body to a risk of toxicity [14].

All this shows how dangerous Pb^{2+} is to the human body, and in view of that it is imperative to check the torrents of waste containing Pb^{2+} before pumping it into the water resources. And reduce its percentage to the limit declared by the World Health Organization (WHO) for Pb^{2+} in drinking water (0.05 ppm) [12]. Lead contamination of water occurs as a result of corrosion of pipes used in the water distribution system [15].

1.3 The Concept of Water Purification

Some of the methods currently available to treat and purify water from heavy metals are sedimentation, membrane filtration, reverse osmosis, adsorption, and stabilization. It should be noted that the purification process must be economically viable and sufficient to meet current environmental laws. Adsorption has received great interest over the past decade because it is attractive to remove heavy metals at very low concentrations. Various adsorbents such as chitosan, chitosan triphosphate, modified lignin and kaolinite clays have been reported to remove heavy metals from the aqueous medium [16].

Many methods have been devised to purify water from impurities and pollutants that made it unsuitable for drinking or irrigation. Methods of water purification generally depend on some scientific basis, including the use of ultraviolet rays for disinfection, filtration to remove solid plankton, removal of water hardness, the application of the reverse osmosis process in Sea water desalination, ion exchange, adsorption (using activated carbon), membrane separation, ozone, crystal freezing, membrane purification and light-based chemical techniques (photochemical processes) [17].

Most of these methods are successful in wastewater purification, while others may be of limited use due to their ineffectiveness or excessive cost. For example, physical filtration of solid particles is not beneficial for its use at low concentrations [9]. Adsorption by ion exchange using activated carbon is an awfully expensive process due to the need to recharge the activated carbon, in addition to disposal of a large amount of the solution. The membrane technique is very expensive because the membranes are subjected to contamination and damage by germs [17]. There are other methods that require high costs to apply.

The methods used in wastewater purification must be feasible and achieve a high removal rate with the lowest operational costs in terms of materials, manpower and equipment, the possibility of repeated use, the possibility of benefiting from the pollutants that have been separated, and the energy, resulting in a few wastes of consumable materials that require disposal. New burdens and also the advantage of the purification method is the

ability to remove heavy metal ions to a level below the applicable regulatory standards [18].

Due to this, adsorption process may be the most attractive method due to its economic effectiveness and easy application, making it the most suitable method for its ability to meet the above mentioned criteria [19].

1.3.1 Adsorption

The adsorption process is known as the phase transfer ability that occurs at solid gas or solid liquid interfaces. It is the accumulation of chemical particles on the surface of a solid. During the adsorption process, gaseous or liquid particles adhere to a solid surface and then bind to it via physical and/or chemical reactions. In adsorption science, the solid surface on which the adsorption process takes place is called adsorbent, and the material that is adsorbed on the solid surface is called as adsorbate [20].

In recent years, the adsorption process used in many fields, including wastewater treatment, has caught the attention of many researchers in the environmental community.

The activated carbon was mainly used for the application of the adsorption process in wastewater purification. There are many other good adsorbents such as silica gel, acid slurry, agricultural residues (Jest) and metal oxides [20]. For the material used for adsorption to be attractive, it must have a large (porous) surface area. There is a direct relationship between the surface area of adsorbent and the number of particles that will bind to that surface.

Specific surface area is the surface area available for adsorption per gram of adsorbent material. It can also be affected by factors such as concentration of sorbents, pH, temperature, adsorbate concentration and time [21].

In general, there are four main steps involved the adsorption process: [20]

1. Transfer of ions from the contaminated solution to the adsorbent surface.
2. The adhesion of ions and molecules and their interaction with the surface of the adsorbent.
3. Transportation within adsorbent sites.
4. Separation of adsorbed ions and particles from the adsorbent surfaces (with a view to repeated use).

1.3.2 Classification of Adsorbents

Given the nature of the surface forces, adsorption can be classified into decomposition (physisorption) and chemical adsorption (chemisorption).

In the process of decomposition (physisorption), the main reaction force is Van Der Waals type (weak forces). It is an energy-repellant process whose enthalpy value ranges (25.0-50.0 kJ/mol). It is a reversible process because the value of activation energy (ΔE) is low, and the reverse adsorption is inversely proportional to the temperature ; While in chemical adsorption, The enthalpy of this type of adsorption is relatively high (90.0-250.0 kJ/mol) [23]. And it is directly proportional to the temperature. Here, it should be recalled that chemical adsorption only occurs if there is a chemical bond

between the adsorbate and the adsorbent. This makes chemical adsorption stronger than physical adsorption. Chemical adsorption can be used to selectively remove toxic trace substances from aqueous solutions and is limited to single-layer coverage. Accordingly, the adsorbent material is difficult to regenerate or reuse. On the other hand, the physical adsorption can form multiple layers thus providing more adsorption capacity [23].

There are standards for the quality of the adsorbent material, generally include: [24]

1. High adsorption efficiency and effectiveness: The adsorption activity is strongly dependent on the surface area of the bond, the chemical nature of the adsorbent, and the radius of the pores.
2. High selectivity: It is considered an important factor in separating the components of certain types of mixtures.
3. Adequate adsorption kinetics: The adsorption rate may be fast enough or can be controlled by some applications.
4. Attractive mechanical properties: In order for the adsorbent material to be attractive, it must be mechanically stable and has a large density to resist corrosion and fracture during the adsorption process because it is often exposed to harsh chemical and thermal conditions.
5. Stability and repeatability: a good adsorbent material should be as stable as possible to ensure long life and reliable use.

Recently, the attention of researchers in the field of wastewater purification has tended to harness the properties of polymer materials in the field of adsorption, as they have large surface areas that are sufficient for the purpose [25]. These features enable us to use these materials to effectively remove toxic heavy metal ions from polluted water. In this study, cellulose loaded with functional amine groups will be synthesized and used in extracting ions of some minerals such as copper and lead from an aqueous solution, where we will load 1-Phenyl biguanide onto cellulose after oxidizing it by sodium periodate.

1.4 Cellulose

Cellulose is available in plants, algae, marine animals, and prepared by some bacteria [26, 43] like *Acetobacter xylinum*, *Gluconacetobacter swingsii* sp., *Acetobacter lovaniensis* HBB5, *Sarcina*, and *Agrobacterium* [27, 44]. It is one of the most abundant natural materials, and it has many properties that make it useful in wastewater purification processes, the most important of these advantages is that it is cheap, available, safe and biodegradable making cellulose polymer environmentally friendly.

Cellulose is one of the widely used natural materials; it has unrestrained number of manufacturing implementations. It interacts like alcohol and it can be transformed into multi polymers with multi implementations.

In this research project cellulose will be prepared, which we will conduct the study on, from the solid waste of the olive industry by a chemical process that was developed at the laboratories of An-Najah National University-

Palestine. Olive process generates two types of waste, the first is a black sticky liquid waste called (Zebar), and the second is solid waste called (Jeft). Effluent contains bio-oxygen (BOD) and also a high percentage of chemical oxygen (COD), in addition to a large proportion of toxic polyphenols [25].

The problem of disposal of olive mill waste is one of the most prominent challenges facing the environment and a source of concern for researchers concerned with protecting the ecosystem from pollution. Studies indicate that the risks of olive industry waste are 100 times higher than the pollution effects of wastewater resulting from domestic uses in urbanized cities, and that the consequences of indiscriminate disposal of these wastes contribute to soil damage and deterioration of its quality and vegetation cover.

In some areas, solid waste is spread on the soil and exposed to the sun until it dries up and then used for heating, resulting in carbon dioxide gas that rises to the layers of the atmosphere, while liquid oil is disposed of through the sewage network, which negatively affects the ecosystem. Therefore, it is imperative to find ways to exploit these pollutants and convert them into useful materials that support the economy of agricultural areas.

1.4.1 Cellulose Structure

Cellulose is a linear polymer formed by the binding of many glucose molecules (D-glucose) that connect with each other in a long unbranched chain and take parallel positions that make the bonds between them very strong and the monomers are linked by β -1,4-glycosidic bonds to form a polymeric chain (Fig. 1.1).

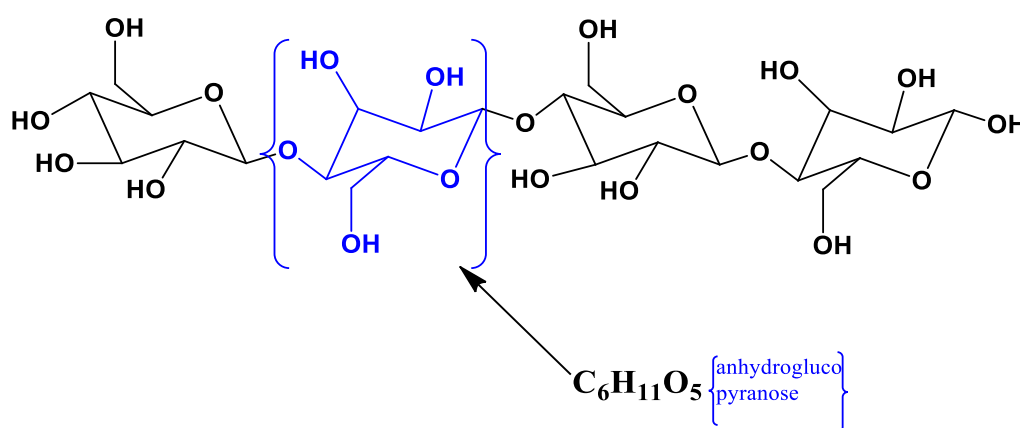


Figure 1.1: Cellulose structure

Each D-anhydroglucopyranose unit carries hydroxyl groups distributed over three sites in the ring of the glucose molecule, so cellulose behaves as alcohol in many of its reactions [29,26].

1.4.2 Related research

Cellulose is of great importance in the field of purifying wastewater from toxic ions. In one research, a chelating group of cellulose loaded with methylbenzalaniline was prepared. The polymer was used to remove copper (Cu^{2+}) and lead (Pb^{2+}) ions from a sample prepared from solution of these

ions. The adsorption kinetic parameters fitted well to the pseudo-second-order kinetic model [27].

In another research, microscopic spheres were synthesized from cellulose and polyethylene loaded with glutaraldehyde. This product was used to study its effectiveness in removing lead ions from a solution prepared with certain concentrations of lead ions, depending on adsorption kinetics and isothermal equations. It was found that the ability of this product to adsorb lead ions is equivalent to approximately 9.46 mg/g, which exceeds the capacity of adsorbing microspheres cellulose by about 50.0% [33].

For the same purpose, cellulose ester was prepared from cheap natural cellulose, and the efficacy of this product in removing copper ions from wastewater was studied. Distinctive results were obtained by using cellulose ester to adsorb copper ions from an aqueous solution prepared for 50.0 minutes and a pH [4.0-5.0] at room temperature [30].

Cellulose modified with thiosemicarbazide group was evaluated as an adsorbent for Hg^{2+} from water, the results demonstrated that the thiosemicarbazide modified cellulose possessed high performance for Hg^{2+} adsorption from water with an adsorption capacity of 500.0 mg/g. The sorption model followed Langmuir model and pseudo-second order kinetic model. The fitting coefficient (R^2) was more than 98%. The enhanced Hg^{2+} adsorption capability of thiosemicarbazide modified cellulose was related to chelating interaction between Hg^{2+} and thiosemicarbazide [31].

In this work, we will prepare and evaluate new cellulose modified with an aromatic amine cleaning agent that has the ability to extract toxic metal ions from wastewater. The cellulose chosen for this work is nanocrystalline cellulose (NCC).

1.4.3 Nanocrystalline Cellulose (NCC)

Recently, nanotechnology has been employed to develop a new generation of attractive materials with high and distinctive performance. Some researchers in the field of nanotechnology science have been able to employ some materials that have the nanoscale characteristic in the field of industry, such as the use of nanoparticles and metal nanooxide particles to improve the performance and the quality of the adhesive materials for wood [32]. Also, activated carbon was used as a filter for water pollutants.

However, some problems have emerged that threaten the environment because of the use of such materials, in addition to the fact that this type of particles is expensive and difficult to regenerate. These problems have drawn the attention of researchers to the discovery of cheap, environmentally friendly, and renewable nanomaterials. The cellulose polymer showed its possession of the nanoscale property, which is the main component of wood, so it is highly abundant in the surrounding environment, and these features made it an attractive material that can be employed in the field of nanotechnology.

Cellulose is made up of different hierarchical microstructures called nano-sized microfibrils. These fibers contain crystalline regions such as

nanocellulose and amorphous regions such as lignin and hemicellulose [32]. The crystalline region was called a nanocellulose or nano whisker [33]. The amorphous zone is removed to isolate the crystalline parts and produce nanocrystalline cellulose (NCC) from normal cellulose through the strong acid hydrolysis process.

However, the use of strong acid solutions may affect the structure of the crystalline fractions, the thermal stability, and the surface shape of the fibers. Therefore, some research has been done to improve the crystallinity and thermal stability during the isolation of NCCs, such as research conducted by Deepa and other scientists [34]. The crystal parts in this variety of cellulose have a diameter of about (0.003-0.01 μm) and a length of (0.1-0.3 μm), a high area of about (100.0-160.0 m^2/g), a high form factor of about 70 and a density of about (1.4 g/cm^3) [35], which makes them very durable as styrene-latex-acrylate, starch, polyhydroxybutyrate or poly (ethylene oxide) octanoate [33, 34].

There are many sources of NCC such as hard and soft wood fibers, wheat straw, sisal, pineapple leaves, coconut husk fibers, berries, bananas, sugar cane, bamboo, jute, rice straw, eucalyptus wood, soybean hull, cotton linter and eucalyptus [34].

After conducting this study, it is expected that we will succeed in employing nanocrystalline cellulose (NCC) in the field of adsorbing toxic metal ions from wastewater, thus saving water consumption and maintaining a clean healthy environment. The main objective of this research is to develop

effective, durable, inexpensive and environmentally friendly materials in the field of wastewater purification. The effect of using NCC will be shown on the mechanical properties, morphology and thermal stability of the product.

1.4.4 1-Phenylbiguanide (PBG)

1-Phenylbiguanide is classified as bioguanides in which one last nitrogen atom is replaced by a phenyl group. It has several synonymous names such as (PBG, Phenyl diguanide, N-phenylbiguanide, N-phenyl-N⁻-guanidine), Its molecular formula is (C₈H₁₁N₅) and its atomic mass is 177.2 g/mol. It was employed in the study of the role of serotonin receptors in the central nervous system as it is an agonist for 5-hydroxytryptamine receptors [37], in addition to its ability to increase hormone secretion Dopamine from the nucleus cells of recumbent mice found in the brains of living organisms [36].

1.1.1 Phenylbiguanide has been exploited in the preparation of various heterocyclic compounds , as it has been used to prepare amanozine. Figure 1.2 shows the structural structure of Phenyl biguanide.

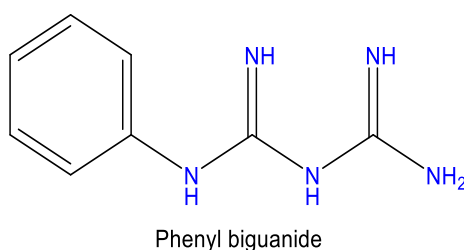


Figure 1.2: Phenyl biguanide structure

In this study, NCC was prepared and then biguanide was attached to it to form a modified 3-D cross-linking cellulose to improve the ability to extract toxic metals from polluted water.

Scope of the work

The main objective of this study is to develop a novel natural based adsorbent for toxic metals from wastewater.

The sub objectives of this research project are to:

- Convert cellulose extracted from Jift to NCC.
- Develop a chemical method to oxidize NCC
- Derivatized the oxidized NCC with an amine containing multi binding sites for metals.
- Evaluate the efficiency of prepared cellulose-based amine as a metal adsorbent and use it in wastewater purification.

Chapter Two

Experimental

2.1 Instrumentation

The instrumentations used in the current research include: shaking water bath (Daihan Labtech, 20.0 to 250.0 rpm Digital Speed Control), pH meter (JENWAY, 3510), Flame Atomic Absorption Spectrometer, Inductively Coupled Plasma Mass Spectrometer ICP-MS (ICE 3xxx C113500021 v1.30) and FT-IR Spectrometer (Thermo Fisher Scientific, Waltham, MA, USA) and equipped with the Smart Split Peaks Hemi Micro ATR accessory (International Crystal Laboratories, Garfield, NJ, USA).

2.2 Materials

The reagents, solvents and chemicals used in this study were documented with all their analytical specifications and their method of use as they were received without any modification. All reagents were purchased from Aldrich Chemical Company. The reagents include phenylbiguanide, sodium borohydride, sodium periodate.

All solutions were prepared using distilled water. Cellulose used in this study was extracted from the solid waste (Jeft), obtained from the olive industry, by a chemical process that was developed at the laboratories of An-Najah National University, Nablus-Palestine [38].

2.3 Methods

The functional groups of the produced polymers were checked by Fourier transform infrared spectrometry (FT-IR), which were recorded on a Nicolet 6700 FT-IR spectrometer. The following parameters were used: resolution was 4.0 cm^{-1} , spectral range was 600 cm^{-1} to 4000.0 cm^{-1} and number of scans was 128.

The Copper (Cu) ion and Lead (Pb) ion solution concentrations studied in this work were measured by Flame Atomic Absorption Spectrometer (FAAS) to determine residual ions concentration. All analyses were accomplished by three runs and the mean of the three trials was reported. The metal ions concentrations of the real sewer samples before and after treatment were measured by Inductively Coupled Plasma Mass Spectrometry (ICP-MS).

2.3.1 Converting cellulose to nanocrystalline cellulose (NCC)

A process for preparing cellulose powder from solid waste of the olive industry OISW was developed at the laboratories of An-Najah National University, Nablus, Palestine [38]. The cellulose powder extracted from the solid waste of the olive industry (Jeft) was transformed into nanocrystals of cellulose as follows: Initially, 5.0 g of the cellulose powder were added to 200.0 mL of distilled water and stirred by a magnetic stirrer for one hour for activation. Then, 20.0 g of concentrated H_2SO_4 were added to the mixture to

produce a solution with 10.0 % (w/w) H_2SO_4 . The mixture was stirred at 60.0°C for 120.0 minutes. The hot mixture was diluted with ice cold distilled water. The colloidal suspension was centrifuged at ten thousandth rpm and decanted. A 100.0 mL of distilled water was added to the solid residue, mixed, then centrifuged and decanted. The process was repeated three times to completely remove the sugar hydrolysis product and the sulfuric acid.

2.3.2 Oxidation of Nanocrystalline Cellulose (NCC)

Initially, cellulose was oxidized to a dialdehyde: a sample of microcrystalline cellulose was added with a mass (10.0 g) equivalent to 0.062 mol of the anhydrous glucose repeating unit and an excess of NaIO_4 (20.0 g, 0.093 mol) into 500.0 mL of distilled water in a beaker (1.0 L). The beaker containing the mixture was covered with aluminum foil (in a dark room), then the container was placed in a hot water bath at a temperature of 40.0°C with stirring by a mechanical mixer for 24.0 hours, after which the sediments were filtered and collected by vacuum filtration (a separating funnel). The collected precipitate is the oxidized cellulose (dialdehyde).

2.3.2.1 Extent of oxidation

A 1.0 g sample of the oxidized cellulose was added to 50.0 mL of 2-propanol. After stirring the suspension for 10.0 minutes, 10.0 mL of distilled water were added. The pH of the mixture was adjusted to 3.5 using a dilute solution of HCl . The mixture was then stirred for another 30.0 minutes.

An aqueous solution of hydroxylamine hydrochloride ($\text{NH}_2\text{OH}\cdot\text{HCl}$, 5.0% by mass) was prepared by dissolving 1.0 g of hydroxylamine hydrochloride in 20.0 mL of distilled water. The pH of the solution was adjusted to 3.5 using a dilute solution of HCl.

The hydroxylamine hydrochloride solution was added to the oxidized cellulose suspension and stirred for 5.0 hr. Then it was titrated with 0.5 N NaOH solution to a pH 3.5 end point.

The following equation was used to calculate the aldehyde content:

$$[\text{Ald}] = (V_{\text{NaOH}} N_{\text{NaOH}} * 162) / W_{\text{OC}} \quad \text{Eq. 1}$$

Where; [Ald]: the aldehyde content (mmol/anhydroglucose repeat unit).

V_{NaOH} : the volume of NaOH (mL) used in the titration.

N_{NaOH} : the normality of the NaOH (eq/L).

W_{OC} : the dry weight of oxidized cellulose (g) used in titration.

2.3.2.2 Derivatization of Cellulose Dialdehyde

Cellulose aldehyde prepared as shown before was converted into modified cellulose by reacting it with 1-phenylbiguanide to prepare the first adsorbent polymer (NCC-PBG-A) that carries imine and amine functional groups. The cellulose based amine NCC-PBG-A was prepared as follows: 1.0 g (0.0062 mol) of oxidized cellulose powder and 1.0 g of phenylbiguanide (0.0056 mol) were added to a 50.0 mL of methanol as solvent in a 100.0 mL round bottom flask. The flask was connected to a condenser to ensure that methanol

remains in the reaction flask during heating. The round bottom flask containing the mixture was placed in an oil bath heated at about 70.0°C for a period of 24.0 hrs.

After heating was completed, the product appeared as a precipitate at the bottom of the flask.

Procedure A was repeated exactly, except that 1.0 mL of acetic acid was added as a catalyst to the reaction mixture. The polymer was separated from the solution by simple filtration after being cooled.

2.3.2.3 Reduction of NCC-PBG-A

The reduction of NCC-PBG-A was accomplished by the addition of 0.3 g of sodium borohydride to a solution of NCC-PBG-A (1.0 g in 30.0 mL of methanol) in a round bottom flask. The reaction mixture was stirred at room temperature for 24.0 hr. The polymer NCC-PBG-B was separated from the solution and collected by simple filtration.

2.4 Preparation of Standard Solutions

Lead (Pb^{2+}) stock solution (1000.0 ppm) in distilled water was prepared by dissolving 0.15985 g of $\text{Pb}(\text{NO}_3)_2$ (331.21 g/mol) in a 100.0 mL volumetric flask. Several standard solutions of lead Pb^{2+} with different concentrations (1.0, 5.0, 10.0, 15.0, 20.0 ppm) were prepared by dilution from the stock solution.

Copper ion (Cu^{2+}) stock solution (1000.0 ppm) was prepared by dissolving 0.2683 g of $\text{CuCl}_2 \cdot 2\text{H}_2\text{O}$ (170.48 g/mol) in distilled water and then diluting to the volume of a 100 mL volumetric flask. Several standard solutions of Cu^{2+} with different concentrations (1.0, 5.0, 10.0, 15.0, 20.0 ppm) were prepared by dilution from the stock solution.

The standard solutions were used in batch experiments for studying the effect of various factors such as: initial concentrations, time, pH, dosage and temperature on the effectiveness of the adsorption process.

Based on flame atomic adsorption spectroscopic (FAAS) measurements and the resulting calibration curves, the copper and lead ions concentrations in the samples were calculated.

2.5 Calibration Curves

Flame atomic adsorption spectroscopy (FAAS) was used to create the calibration curves for Cu^{2+} and Pb^{2+} ions by measuring the absorbency of the standard solutions.

The calibration curves for Lead Pb^{2+} and Copper Cu^{2+} are shown in Figures 2.1 and 2.2, respectively.

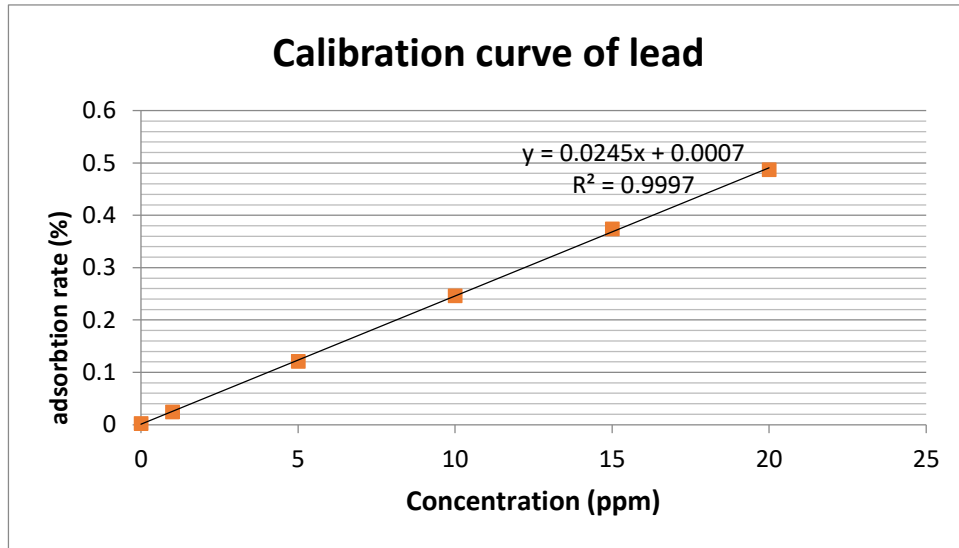


Figure 2.1: Calibration curve of lead Pb^{2+}

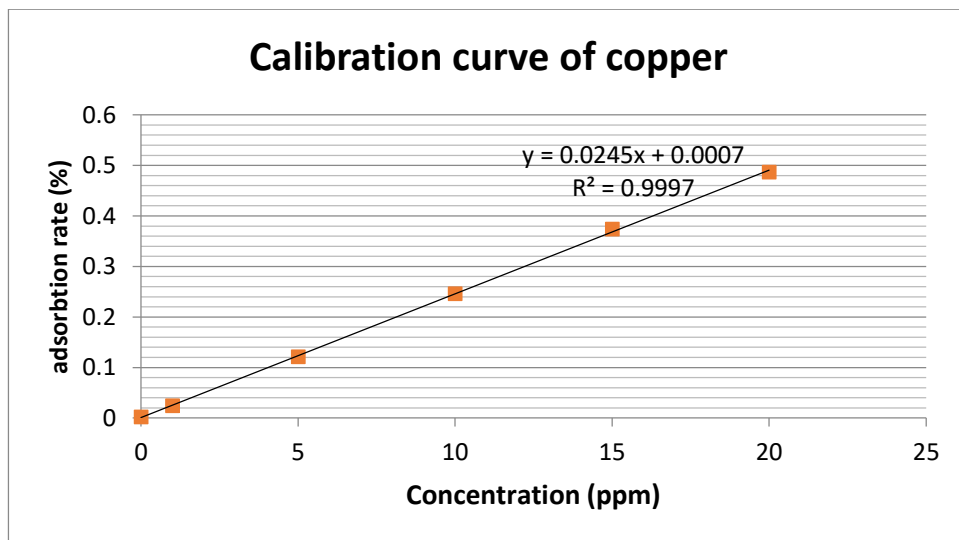


Figure 2.2: Calibration curve of copper Cu^{2+}

2.6 Batch Adsorption Experiments

A sample with known mass of (NCC-PBG-A) or (NCC-PBG-B) was added to a specified volume of a standard solution of the heavy metal Cu^{2+} or Pb^{2+} and agitated. The effect of solution conditions including amount of prepared adsorbent, time, temperature, pH value and metal ion initial concentration

were studied. Atomic adsorption measurements of the filtered mixture were made for each sample to calculate the residual concentration of the metal ion and thus to evaluate the efficiency of the adsorption.

2.6.1 Effect of Adsorbent Weight (Dosage)

For determining the optimum amount of adsorbent in the adsorption of Cu^{2+} and Pb^{2+} on modified cellulose, 5.0, 10.0, 50.0, 75.0 or 100 mg of the modified cellulose was added to five vials containing 10.0 mL of 20.0 ppm standard solution of the metal ion. The mixtures were placed in a shaking water bath at a constant temperature of 25.0°C , and a pH 7.0 for 10.0 minutes.

Then, the concentration of the metal ions in the filtrate was determined by FAAS.

The results obtained for the effect of the weight of dosage NCC-PBG-A and NCC-PBG-B for the adsorption of both copper Cu^{2+} and lead Pb^{2+} ions are shown in Table 2.1 and are graphically represented in Fig. 3.7 & 3.12, Respectively.

Table 2.1: Effect of the Wt. of dosage of NCC-PBG-(A & B) for the adsorption of both Cu²⁺ and Pb²⁺ ions.

	NCC-PBG-A		NCC-PBG-B	
	Percentage of removal (%)			
Wt. of Dose (mg) \ Ions	Cu ²⁺	Pb ²⁺	Cu ²⁺	Pb ²⁺
5.0	55.5	87.2	83.9	97.5
10.0	68.9	93.5	90.1	97.9
50.0	75.4	95.9	95.9	99.5
75.0	69.9	94.8	96.8	99.3
100.0	77.8	95.7	97.3	99.3

2.6.2 Effect of Adsorbate Concentration

In order to find out the optimum concentration of lead Pb²⁺ and copper Cu²⁺ ions, the optimal dose (100.0 mg) of each polymer was added to five flasks, each containing 10.0 mL of different standard concentrations of Cu²⁺ & Pb²⁺. The pH 7.0, time 10.0 min and temperature 25.0 °C were kept constant for the five samples. Next, the metal ion concentration in each filtrate is measured using FAAS.

The results obtained for the effect of the concentrations of adsorption of both copper Cu²⁺ and lead Pb²⁺ ions on the surface of NCC-PBG-A and NCC-PBG-B are shown in Table 2.2 and are graphically represented in Fig. 3.8 and 3.13, respectively.

Table 2.2: Effect of the concentrations of adsorbate on the adsorption of both Cu^{2+} and Pb^{2+} ions on the NCC-PBG-(A & B).

	NCC-PBG-A		NCC-PBG-B	
	Percentage of removal (%)			
<i>Ions</i> Conc. (ppm)	Cu^{2+}	Pb^{2+}	Cu^{2+}	Pb^{2+}
1.0	76.9	95.9	95.7	99.2
5.0	70.8	95.7	97.8	98.4
10.0	72.1	96.3	91.8	99.5
15.0	69.7	93.8	93.0	99.8
20.0	65.5	94.0	91.5	99.0

2.6.3 Effect of Time

The adsorption of the metal ions on each adsorbent was studied as a function of contact time at the optimum dosage of polymer and adsorbate concentration. A sample of the 20.0 ppm standard solution at pH 7.0 was placed in a volumetric flask and shaken with 10.0 mg of the polymer. At the end of each time interval (1.0, 5.0, 10.0, 15.0 and 20.0 min), each sample was filtered off and the concentration of the metal ion was measured by FAAS.

The results obtained for the effect of the contact time for NCC-PBG-A and NCC-PBG-B on the adsorption of both Cu^{2+} and Pb^{2+} ions are shown in Table 2.3 and are graphically represented in Fig. 3.4 and 3.9, respectively.

Table 2.3: Effect of the shaking time on the adsorption of both Cu^{2+} and Pb^{2+} ions on the NCC-PBG-(A & B).

	NCC-PBG-A		NCC-PBG-B	
	Percentage of removal (%)			
<i>Ions</i> Time (min)	Cu^{2+}	Pb^{2+}	Cu^{2+}	Pb^{2+}
1.0	35.9	78.4	61.0	97.9
5.0	52.8	93.8	82.2	95.5
10.0	65.1	92.4	91.0	98.8
15.0	65.5	90.7	91.2	98.2
20.0	64.9	89.6	91.0	98.2

2.6.4 Effect of pH value

Adsorption was studied at various pH values ranging from 2.0-12.0 in order to investigate the effect of pH on the adsorption process. The required pH values were obtained by using either 0.1 M HCl or 0.1 M NaOH solutions.

The optimum conditions of time, dosage of polymer, and the adsorbate concentration were used for each pH value. 10.0 mg of the adsorbent were added to 10.0 mL of the 20.0 ppm standard solution at a constant temperature of 25.0°C, shaking for 20minute. At the end of each experiment, the samples were filtered off and the concentration of each metal ion was determined by FAAS.

The results for the effect of pH value for NCC-PBG-A and NCC-PBG-B adsorption of both copper Cu^{2+} and lead Pb^{2+} are shown in Table 2.4 and are graphically represented in Fig. 3.5 and 3.10, respectively.

Table 2.4: Effect of the pH value on the adsorption of both Cu^{2+} and Pb^{2+} ions on the NCC-PBG-(A & B).

pH \ Ions	NCC-PBG-A		NCC-PBG-B	
	Percentage of removal (%)			
	Cu^{2+}	Pb^{2+}	Cu^{2+}	Pb^{2+}
2.0	17.1	59.3	38.9	55.6
5.0	23.7	70.9	52.4	76.2
7.0	66.4	93.1	89.8	99.1
9.0	33.1	82.4	68.6	89.4
12.0	23.0	42.4	42.2	78.1

2.6.5 Effect of Temperature

For studying the effect of temperature on the adsorption process, 10.0 mg of the polymer were added to 10 mL of the 20-ppm standard solution of Cu^{2+} or Pb^{2+} ions at a pH of 7.0. Each solution was placed in a shaking water bath at the desired temperature (15.0, 25.0, 30.0, 40.0 and 60.0°C) for the optimum time. At the end of each experiment, the samples were filtered off and the concentration of metal ions was measured by FAAS.

The results obtained for the effect of temperature on NCC-PBG-A and NCC-PBG-B adsorption of both copper Cu^{2+} and lead Pb^{2+} ions are shown in Table 2.5 and are graphically represented in Fig. 3.6 and 3.11, respectively.

Table 2.5: Effect of the temperature on the adsorption of both Cu^{2+} and Pb^{2+} ions on the NCC-PBG-(A & B).

	NCC-PBG-A		NCC-PBG-B	
	Percentage of removal (%)			
Temp.($^{\circ}\text{C}$) \ / ions	Cu^{2+}	Pb^{2+}	Cu^{2+}	Pb^{2+}
15.0	66.0	95.2	83.9	99.2
25.0	68.8	92.5	92.4	98.7
30.0	61.3	90.0	74.8	98.8
40.0	40.7	83.7	58.7	91.1
60.0	25.9	67.4	33.2	79.9

2.7 Adsorption kinetics

The kinetic laws were applied to the results obtained to understand the kinetics of the adsorption process of the metal ions on the modified cellulose polymers, NCC-PBG-A and NCC-PBG-B.

The adsorption kinetics was studied under optimal conditions of contact time, pH, temperature, polymer dosage, and metal ions concentration.

The concentration of metal ions was determined before and after adsorption. The results were studied using Langmuir and Freundlich isotherms.

50.0 mg of the polymer were added to 10.0 mL of a 20.0 ppm of Cu^{2+} solution at pH 7.0 and shaken for 10.0 minutes at room temperature. A sample of a solution of lead ions Pb^{2+} was also studied under optimal conditions for the adsorption of Pb^{2+} . The adsorption rate was measured and compared with

theoretical models. The pseudo-kinetic models of the first and second order were applied to the experimental results at various contact times. Parameters of the pseudo first and pseudo second order kinetic models (K , q_e and R^2) of ions adsorption on both polymers were determined and the calculated and experimental q_e values were compared.

2.8 Adsorption Thermodynamic

It is necessary to study the thermodynamics of the adsorption process in order to evaluate the suitability of such process. The behavior of the adsorption process can be studied by calculating thermodynamic parameters such as the change in enthalpy (ΔH), change in entropy (ΔS) and change in free energy (ΔG).

The relationship among the adsorption parameters is summarized by the following equation [49]:

$$\Delta G = \Delta H - T\Delta S \quad \text{Eq. 2}$$

Where; ΔG : the change in Gibbs free energy (J).

ΔH : the change in enthalpy (J)

ΔS : the change in entropy (J/K)

T: the absolute temperature (K).

ΔG is related to the thermodynamic equilibrium constant (K_d) by the following equation:

$$\Delta G = -RT \ln K_d \quad \text{Eq. 3}$$

Where, R: the universal gas constant that equals 8.314 J.mol⁻¹. K⁻¹.

K_d: the thermodynamic equilibrium constant that equals (q_e/C_e) with a unit of mol or (L/g).

Substitution of equation 3 into equation 2 and rearrange gives:

$$\ln K_d = \frac{\Delta S}{R} - \frac{\Delta H}{R} \quad \text{Eq. 4}$$

A plot of lnK_d versus ($\frac{1}{T}$) in the Van't Hoff plot gives a straight line with a slope of ($-\frac{\Delta H}{R}$), and a y-intercept equals ($\frac{\Delta S}{R}$).

2.9 Wastewater Purification

A sample of sewer was collected from the sewage system in one of the Palestinian cities for being used in this work. The types and concentrations of metal ions present in the sample were determined by ICP-MS (the analysis was performed by Water Center at An-Najah National University, Nablus, Palestine).

Two 10.0-mL aliquots of sewage water were withdrawn with a syringe, filtered through a syringe equipped with a 0.45 μm filter and placed into two bottles. The optimum conditions for the adsorption on each polymer were applied to each bottle individually. A sample from each mixture was withdrawn with a syringe and filtered through a 0.45 μm syringe filter and subjected to analysis by ICP-MS for the residual metal ions concentrations.

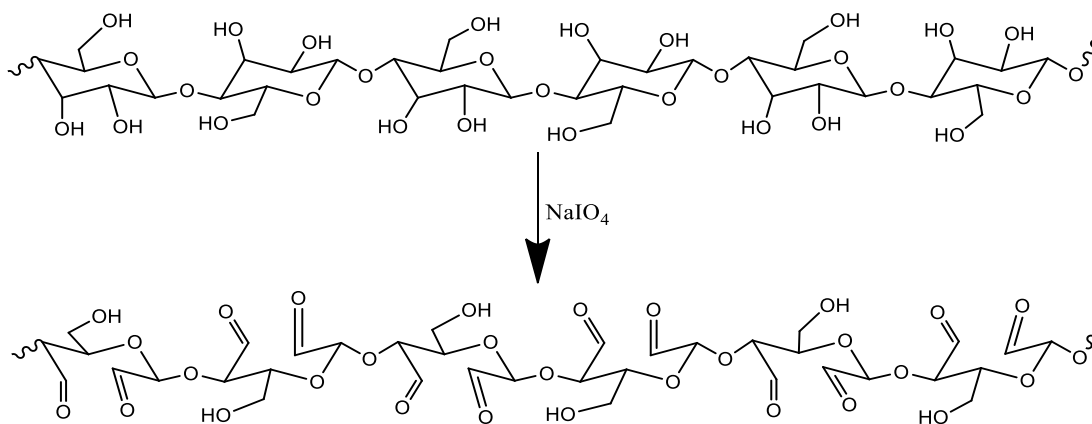
Chapter Three

Results and Discussion

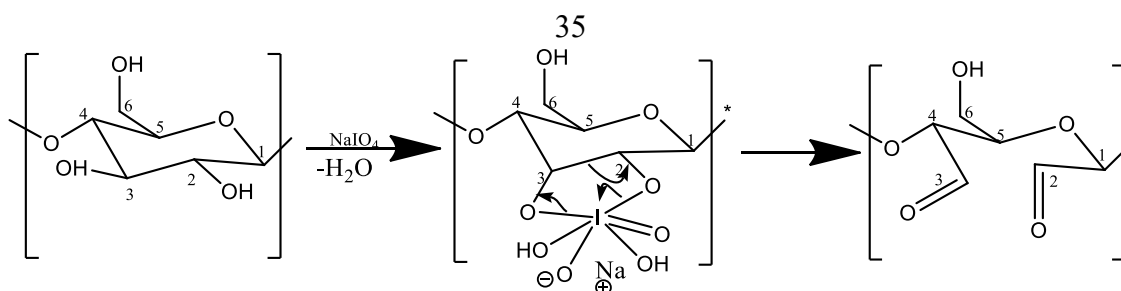
3.1 Oxidation of NCC cellulose to 2,3-Dialdehyde Cellulose

The cellulose was oxidized to a cellulose dialdehyde (OC) by NaIO_4 reagent as shown in Scheme 3.1. It is known that Periodate (IO_4^-) oxidizes a contiguous dihydroxyl group in the cellulose chain to a dialdehydes. The reaction conditions and amount of reagent were optimized to obtain the highest possible yield. This method is known as the Jackson and Hudson method [39,40].

In this method cellulose is treated with an aqueous solution of periodate (NaIO_4) in a system completely isolated from light. Periodate complexes to the vicinal hydroxyl group at C_2 and C_3 which leads to cleavage of C_2 - C_3 bond and oxidation of the vicinal hydroxyl groups to form 2,3-dialdehyde units along the cellulose chains as shown in Scheme 3.1 & 3.2.



Scheme 3.1: Conversion of NCC to cellulose dialdehyde.



Scheme 3.2: Mechanism for oxidation of NCC

3.1.1 Determination of Aldehyde Content

The proportion of aldehyde produced after oxidation of cellulose (dialdehyde) was assessed by using hydroxylamine-hydrochloride [41]. Where, a known amount of oxidized cellulose was converted to oximes by reacting with hydroxylamine-hydrochloride by following the steps described in the previous section. After the completion of the reaction that would produce the hydrochloric acid, the resulting HCl was titrated with NaOH solution at a known concentration 0.5 N to the end point of pH 3.5 and the cellulose content of aldehyde was calculated using Equation 1:

$$[\text{Ald}] = (V_{\text{NaOH}} N_{\text{NaOH}} * 162.0) / W_{\text{OC}} \quad \text{Eq. 1}$$

Under the reaction conditions presented in the experiment, the proportion of aldehyde in oxidized cellulose (W_{OC}) was approximately 1.83/anhydrous glucose replication unit.

3.1.2 Detection of Aldehyde by FT-IR

The FTIR spectrum of the untreated cellulose is shown in Fig.3.1. The spectrum shows a broad peak at 3317 cm^{-1} due to the stretching of the O-H, the peak at 1300 cm^{-1} could be related to the -OH bending vibration [18], the band at 2903 cm^{-1} corresponds to the C-H stretching vibration, the bands at

1055 cm^{-1} could be attributed to C-O-C stretching and the 1430 cm^{-1} are related C-H bending [42].

The FT-IR spectrum of OC is shown in Fig.3.1. The spectrum shows a band at 1715 cm^{-1} cross bonding to the aldehyde carbonyl groups [43]. The aldehyde peak is not very sharp which could be due to hydration and formation of hemiacetals [44]. Since removal of water completely from cellulose requires drying it by leaving it under vacuum for at least 3.0 hours at 105.5°C at 105.0°C.

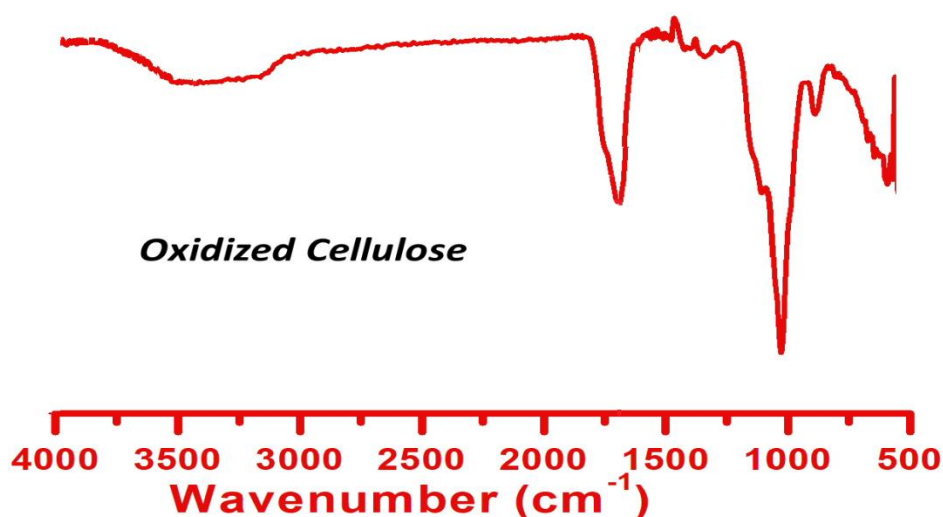


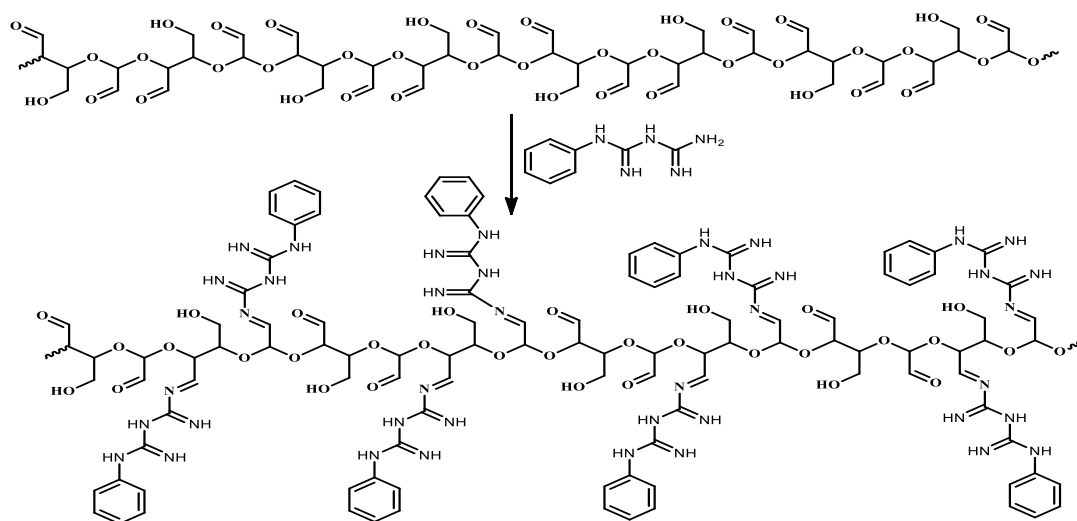
Fig. 3.1: FT-IR spectra of oxidized cellulose (Dialdehyde NCC)

3.2 Cellulose Dialdehyde derivatization with phenylbiguanide

The aldehyde group is known to be versatile; it is very reactive and could be converted to various function group. For example, it can be further oxidized to carboxylic groups [45] or reduced to primary alcohols [46], or reacted with amine to form imine [47]. The imine then could be reduced to an amine. Amine is known to have tendency to complex with metal ions due to its lone

pair of electrons. In this study it was chosen to be converted to an imine then reduced to an amine.

The carbon of the carbonyl group in aldehyde is an electrophilic carbon that undergoes a condensation reaction with the amine as shown in scheme 3.3 to form an imine after losing the water molecule. The figure shows the reaction between dialdehyde nanocrystalline cellulose and phenylbiguanide (PBG). The nucleophilic addition of an amine to the carbonyl complex of the molecule gives rise to an intermediate, followed by donating a proton from nitrogen in PBG to oxygen in carbonyl group of aldehyde, then water is lost to give an polymer (NCC-PBG-A) in excellent yield (> 90%)



scheme 3.3: Crosslinked the NCC (Dialdehyde) with PBG

3.2.1 Detection of Imine in Polymer (NCC-PBG-A) by FT-IR

We note the disappearance of the aldehyde domain at 1728 cm^{-1} and the presence of the imine group $\text{C}=\text{N}$ at about 1675 cm^{-1} and $\text{C}=\text{C}$ of the aromatic group around 1570 cm^{-1} , and we note the emergence of $\text{C}-\text{N}$ at about 1230 cm^{-1} and $\text{N}-\text{H}$ amine in the period $3270\text{--}3480\text{ cm}^{-1}$ in addition to the wide

O-H range that appears in almost the same region, so the N-H amine signal is imprecise, as shown in the figure 3.2 .

Here, we notice that the polymer (NCC-PBG-A) resulting from the process of binding the dialdehyde nanocrystalline cellulose with phenylpyguanide contains original amine groups in addition to the imine group that was produced at the binding site, so we tested the effectiveness of this polymer NCC-PBG-A in removing toxic metal ions before converting the imine into amine and production of the second type of modified cellulose NCC-PBG-B, and the results have been documented and compared, and will be shown later.

Phenylbiguanide was chosen, because it reacts with the aldehyde functional group on the cellulose chains to form a polymer carrying amine groups that are known high affinity for metals and very effective in extracting metals from wastewater.

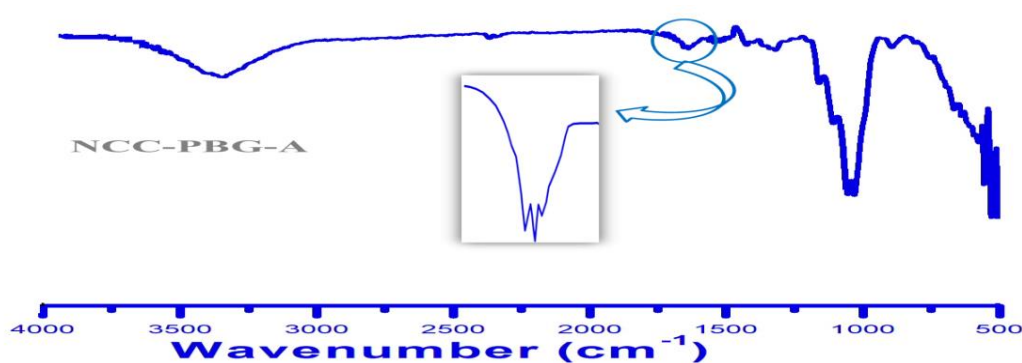
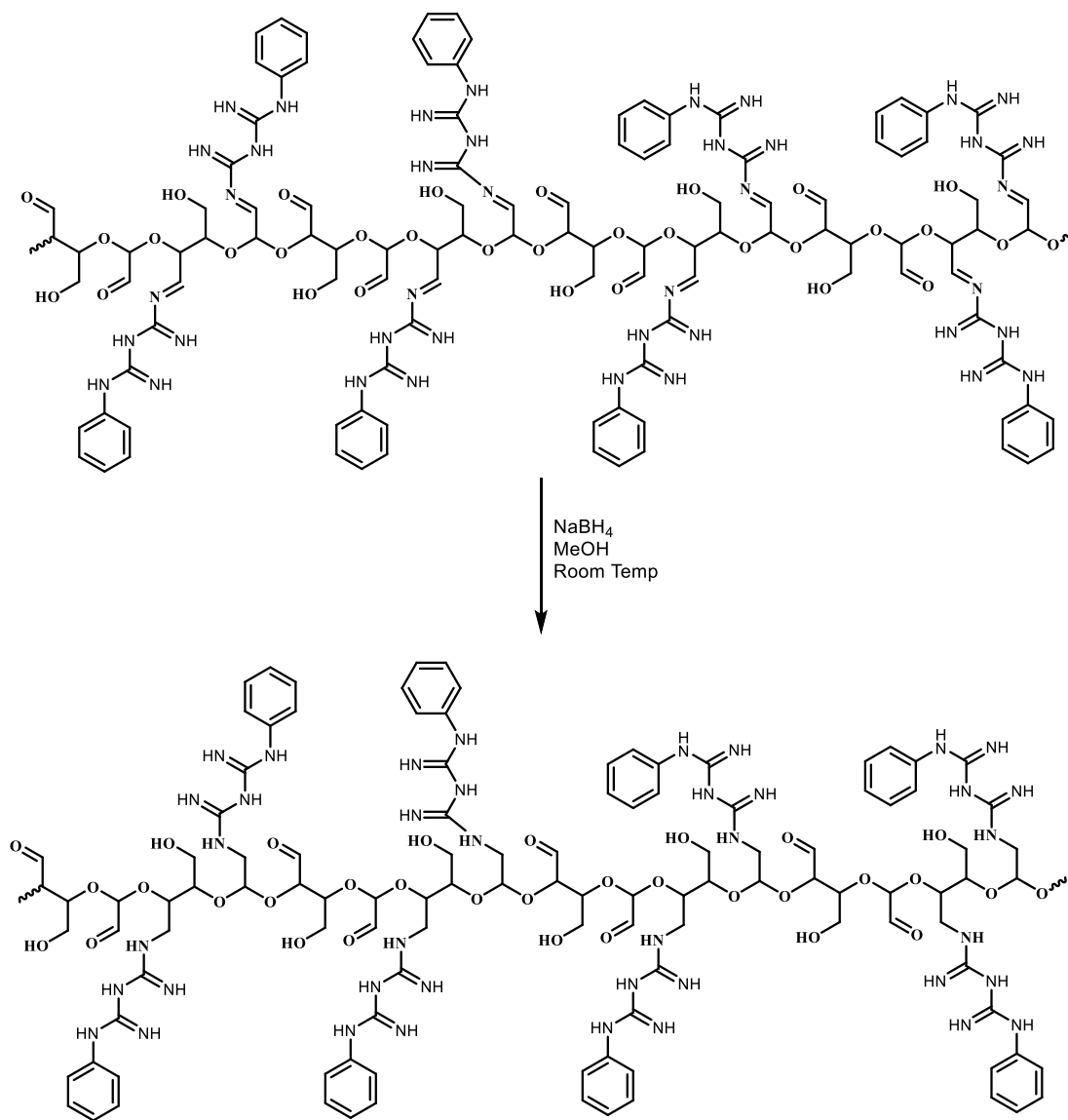


Fig. 3.2: FT-IR spectra of polymer NCC-PBG-A

3.2.2 Conversion of Imine into an Amine by Reduction

The reduction of cellulose imine was carried out with sodium borohydride as shown in scheme 3.3, the reaction was carried out in methanol to prepare the second polymer NCC-PBG-B.



Scheme 3.4: Preparation of the NCC-PBG-B polymer from NCC-PBG-A polymer

3.2.3 FT-IR for Polymer (NCC-PBG-B)

The obtained FT-IR spectrum (figure 3.3) shows the disappearance of the imine band at 1675 cm^{-1} . A signal at 1573 cm^{-1} is shown as an indication of the presence of C=C in aromatic rings as before with the NCC-PBG-A spectrum. The N-H band appeared at about 3300 cm^{-1} , but we note that the signal increased because of the transformation of the imine groups into an amine, and this region appears covered by the O-H band that appears in the same region, so the signal appears to be somewhat wide.

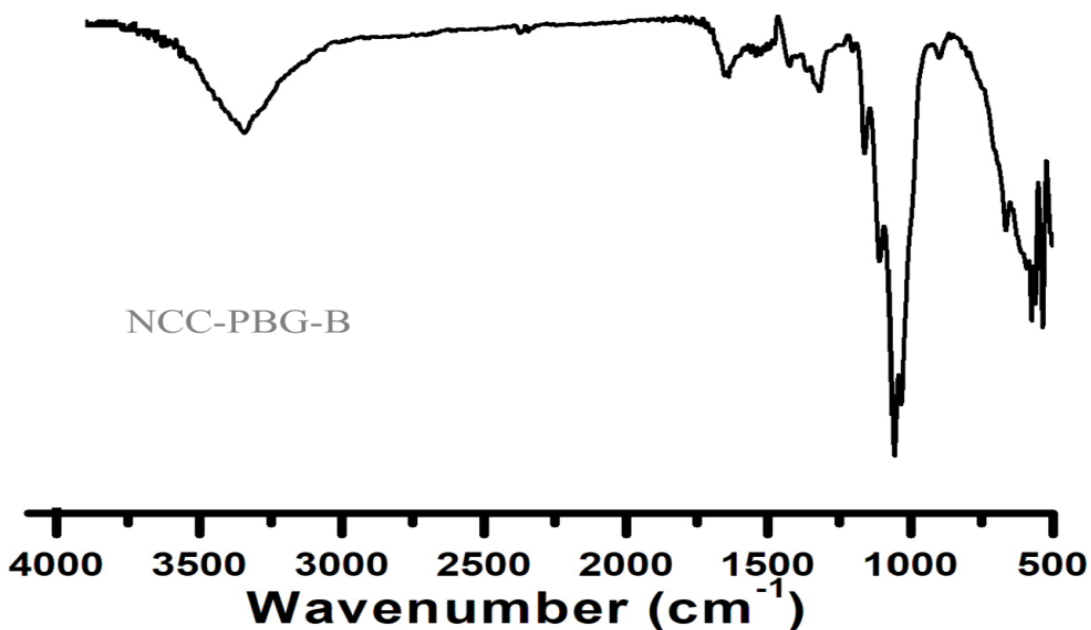


Fig. 3.3: FT-IR spectra of polymer NCC-PBG-B

3.4 Adsorption Results

This research aims to use modified synthetic nanocrystalline cellulose to remove heavy metal ions from wastewater, and to compare the adsorption efficiency of the prepared polymers.

This process was performed by studying the adsorption capabilities of phenylpyguanide-substituted crystalline cellulose towards lead Pb^{2+} and copper Cu^{2+} ions. The extracted concentrations of heavy metal ions were measured using atomic adsorption spectroscopy.

After finding the remaining concentrations, the percentage of removal must be determined for each uptake. This value is defined as the ratio of the difference in the concentration of adsorbates before and after adsorption ($C_i - C_f$), to the initial concentration of the metal ion in the aqueous solution (C_i), as shown in the following equation:

$$\% \text{ adsorption} = \frac{C_i - C_f}{C_i} \times 100\% \quad \text{Eq. 4}$$

Where; C_i : Initial concentration of heavy metal ion in solution (ppm).

C_f : Final concentrations of heavy metal ion in solution (ppm).

The adsorption capacity q_e (mg/g) was measured for different ion concentrations under experimental conditions at equilibrium, as shown in the following equation [48].

$$q_e = \left(\frac{C_i - C_f}{m} \right) * V \quad \text{Eq. 5}$$

Where; V : the volume of solution (L) .

m : the mass of adsorbent (g) .

The adsorption processes are compared by using the same adsorbent with Cu^{2+} or Pb^{2+} ions, or using the same heavy metal with different adsorbents including NCC-PBG-A or NCC-PBG-B.

3.4.1 Adsorption of Copper Ions (Cu^{2+})

The effect of solution conditions for Cu^{2+} adsorption on the adsorbents (NCC-PBG-A or NCC-PBG-B) was evaluated. In this way when changing the polymer, the adsorption dependence on the nature of the adsorbent is investigated.

3.4.1.1 Effect of Contact Time

To determine the optimal contact time for adsorption of Cu^{2+} ions by both adsorbents, the adsorption capabilities of Cu^{2+} were measured as a function of time as shown in (Fig. 3.4).

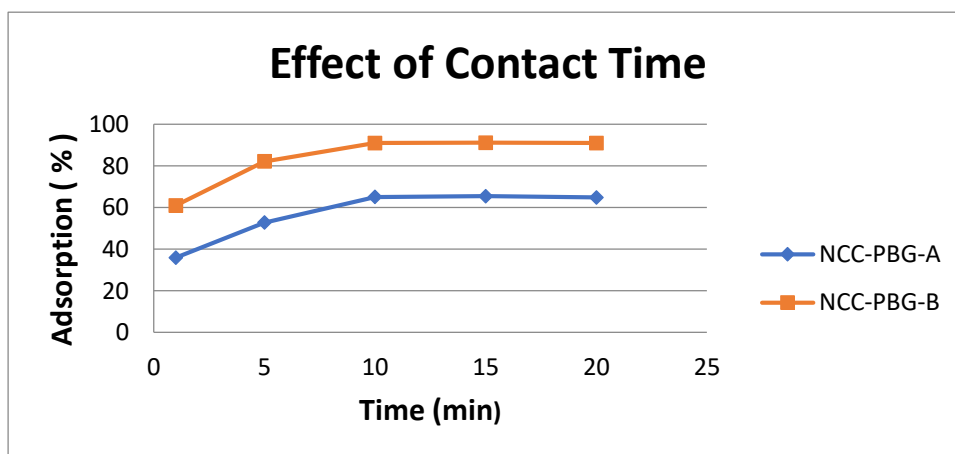


Fig.3.4:Effect of contact time on the adsorption of Cu^{2+} on NCC-PBG-(A & B) ($C_i = 20$ ppm, adsorbent dose = 0.01 g, volume of soln. = 10.0 mL, pH = 7, at room temperature).

This graph shows that the highest percentage of Cu^{2+} removal was for NCC-PBG-B after 10 minutes of shaking as the optimum contact time between adsorbent and adsorbate, and this percentage is approximately 91.0%. Whereas, when using NCC-PBG-A to remove Cu^{2+} ions, the percent of removal was approximately 65.3% after 10 minutes as well.

The residual concentration of copper ions after each optimum contact time becomes almost constant. The high Cu^{2+} percent of removal at the beginning were due to the large availability of binding sites on the outer adsorbent surface. In general, we noticed that the optimum time to adsorb copper ions by both polymers was about 10.0 minutes, but if we look at the effectiveness of each one of them, we notice that the NCC-PBG-B polymer extracts copper ions by 91.0% during this time period, so we can consider that NCC-PBG-B more efficient than NCC-PBG-A to remove Cu^{2+} . This is because amine is more stable than imine and bind stronger to metals.

3.4.1.2 Effect of pH value

One of the most important factors controlling the adsorption of metal ions from aqueous solutions is the pH value because the pH can influence the surface charge of the polar polymers. Figure 3.5 shows the effect of pH on the adsorption efficiency of Cu^{2+} on different adsorbents. These studies were conducted at the optimum contact times 10.0 min of both polymers with a variable pH value of the solution.

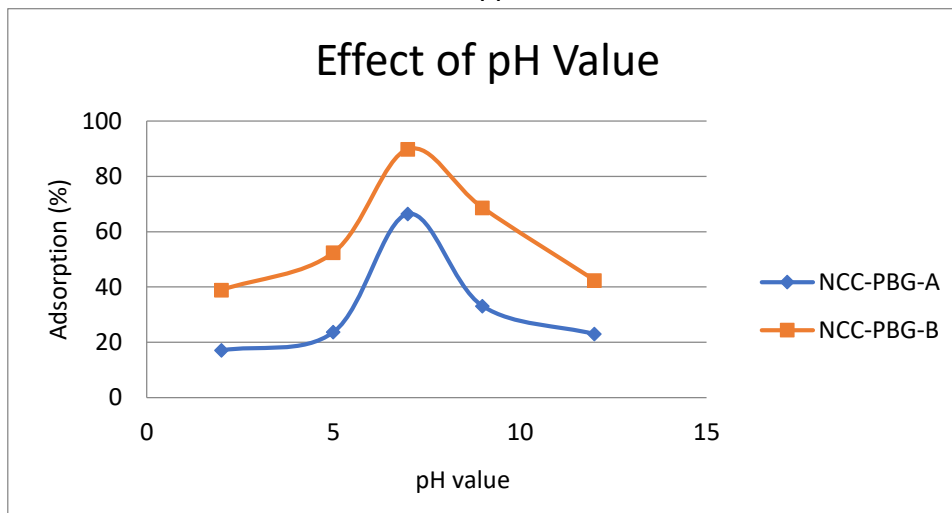


Fig. 3.5: Effect of pH value on the ads. of Cu^{2+} on NCC-PBG-(A & B) ($C_i = 20$ ppm, adsorbent dose = 10.0 mg, volume of soln. = 10.0 mL, For 10.0 min, at room temperature)

For the polymer NCC-PBG-B, the adsorption percentage increases with the pH to reach the maximum at pH 7.0, after which it decreases with further increase in the pH value. This polymer showed a maximum removal percent of Cu^{2+} of 89.8% compared to NCC-PBG-A of 66.4%.

The increase in the percent removal of metal ions with acidification can be explained based on decreased competition between protons and Cu^{2+} ions of the same functional groups and by a decrease in the positive surface charge, which leads to a decrease in the electrostatic repulsion between protons and metal ions. Whereas it would be expected that the decrease in the percentage of adsorption after each optimum pH of both adsorbers was due to the formation of soluble hydroxy complexes which reduced the adsorption efficiency of the adsorption of Cu^{2+} from the aqueous solution.

3.4.1.3 Effect of Temperature

To study the effect of temperature on Cu^{2+} adsorption by using modified nanocrystalline cellulose derivatives. The optimum conditions for contact time and pH value must be observed. In general, the adsorption efficiency becomes very low at high temperature values.

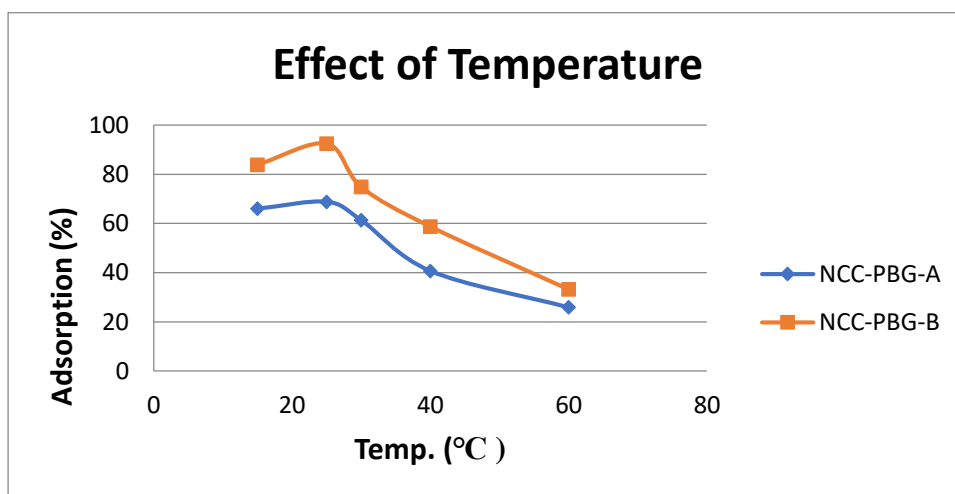


Fig. 3.6: Effect of Temp. on the adsorption of Cu^{2+} on NCC-PBG-(A & B) ($C_i = 20.0$ ppm, adsorbent dose = 10.0 mg, volume of soln. = 10.0 mL, for 10.0 min, pH = 7.0)

As shown in Figure 3.6, it was found that the adsorption of copper ions using both polymers NCC-PBG-A and NCC-PBG-B increases with increasing temperature until a maximum at 25.0°C is reached. After that, the percentage of removal decreases as the temperature is raised. The percentage removal at the optimum temperature value is 67.9% for NCC-PBG-A and 90.6% for NCC-PBG-B. The low temperature of the solution enhances the complexity capacity between the Cu^{2+} ions and both polymers, thus increases the bonding of copper ions with the adsorbent surface, whereas, at higher temperature values, the bonding ability between Cu^{2+} ions and the adsorbent

surface is low. The adsorption process is exothermic; increasing the temperature leads to an increase in the kinetic energy of the adsorbed particles on the adsorbent surface, which leads to an increase in the possibility of their separation from the adsorbent surface.

3.4.1.4 Effect of Adsorbent Dosage

The experimental results of the removal of copper Ions (Cu^{2+}) with respect to the dose of adsorbents NCC-PBG-A and NCC-PBG-B are shown in Figure 3.7 over a range of 5.0 mg to 100.0 mg, at the optimum values for time, pH and temperature.

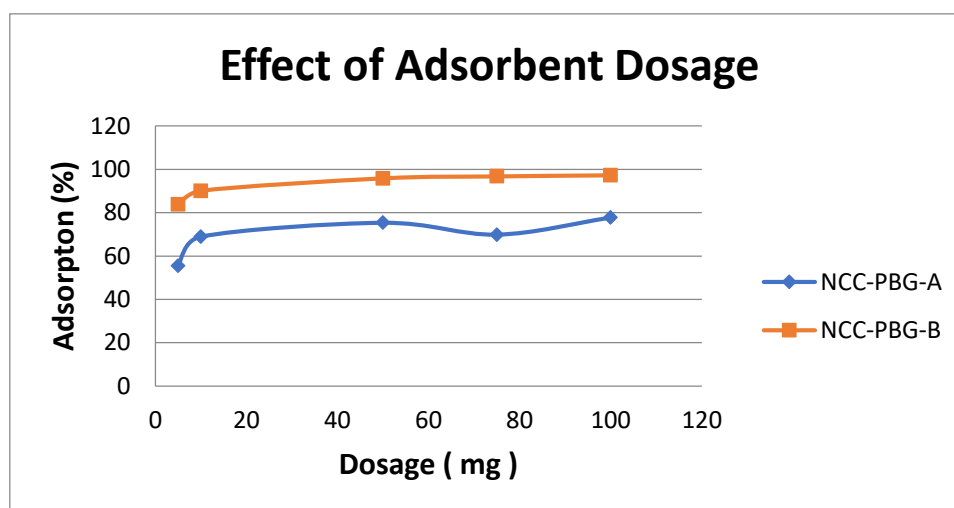


Fig. 3.7: Effect of adsorbent dosage on the adsorption of Cu^{2+} on NCC-PBG-(A & B) ($C_i = 20.0$ ppm, volume of soln. = 10.0 mL, for 10 min, pH = 7.0, at 25.0°C)

The highest removal of Cu^{2+} was 77.8% using 100.0 mg of NCC-PBG-A. The results showed the percentage of removal leveled off at 100.0 mg of adsorbent (Figure 3.7) with an increase in the adsorbent dose. The same relationship between adsorption efficiency and dose effect for

NCC-PBG-B and was 97.3% as percentage of removal. The optimum dose for both polymers is about 100.0 mg.

The increase in the percentage of adsorption of Cu^{2+} ions on the surface of the adsorbents with increasing the dose of the polymers (NCC-PBG-A and NCC-PBG-B) is due to the greater availability of the binding sites of the sorbent materials. Then leveled off once it reached the equilibrium.

3.4.1.5 Effect of Cu^{2+} Initial Concentration

When studying the effect of the concentration of metal ions on the present of removing these ions from aqueous solutions, it was found that the rate of adsorption decreases with the increase in the concentration of these ions in the solution.

The maximum removal of Cu^{2+} ions was 97.8% for NCC-PBG-B using 10 ppm of Cu^{2+} solution. While the optimum concentration for the maximum removal of Cu^{2+} ions by NCC-PBG-A was 5.0 ppm with a percent removal of 76.9%. In general, a decrease in the copper ion concentration results in sufficient adsorption sites to be available for the process (Figure 3.8).

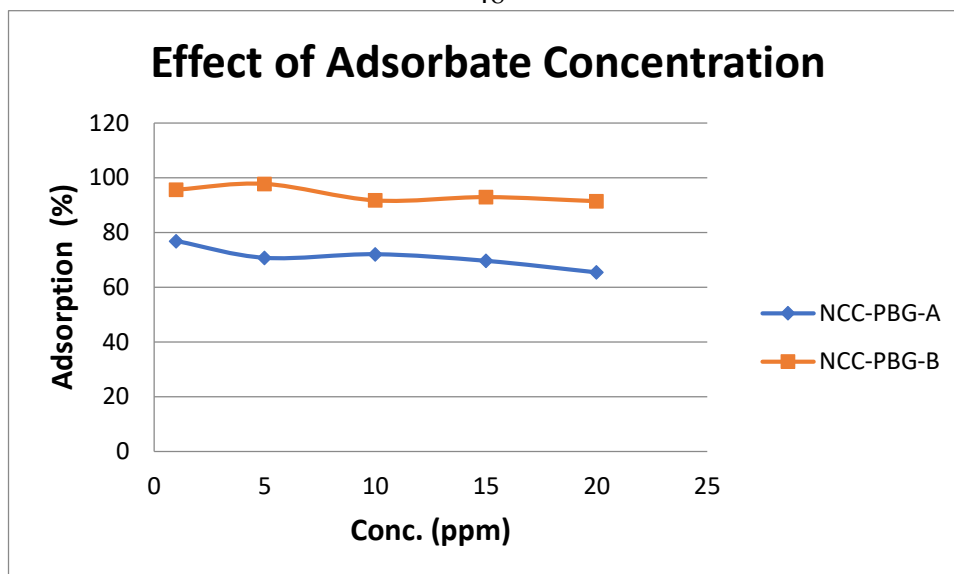


Fig. 3.8: Effect of adsorbate Conc. on the adsorption of Cu^{2+} on NCC-PBG-(A & B) (adsorbent dose = 10.0 mg, volume of soln. = 10.0 mL , for 10 min, pH = 7.0 , at Room Temp.)

The following table (3.1) represents the adsorption results for Cu^{2+} ions from solution using NCC-PBG-A or NCC-PBG-B.

Table 3.1: The adsorption results for Cu^{2+} ions using NCC-PBP-(A & B)

Adsorption of Cu^{2+}		
Optimum Condition and % of Cu^{2+} Adsorption	NCC-PBG-A	NCC-PBG-B
Contact Time (minute)	10.0	10.0
% of Adsorption	65.3%	91.0%
pH value	7.0	7.0
% of Adsorption	66.4%	89.8%
Temperature ($^{\circ}\text{C}$)	25.0	25.0
% of Adsorption	67.9%	90.6%
Adsorbent Dose (mg)	100	100
% of Adsorption	77.8%	97.3%
Adsorbate Concentration (ppm)	5.0	10.0
% of Adsorption	76.8%	97.9%

3.4.2 Adsorption of Lead Ions (Pb^{2+})

The effect of solution conditions on the adsorption lead ions Pb^{2+} on the modified nanocrystalline cellulose polymers (NCC-PBG-A or NCC-PBG-B) was evaluated. When changing the adsorbent polymer, the dependence of adsorption on the nature of the adsorbent is checked.

3.4.2.1 Effect of Contact Time

To study the effect of contact time of lead ions Pb^{2+} on the surfaces of cellulose polymers, the adsorption capabilities of lead ions Pb^{2+} as a function of time were measured (Figure 3.9).

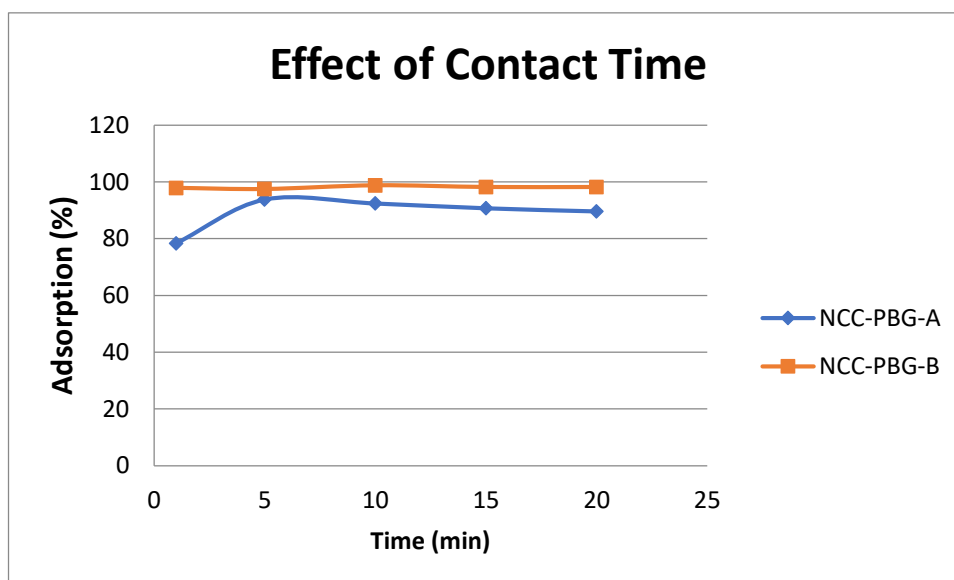


Figure 3.9: Effect of contact time on the adsorption of Pb^{2+} ions on NCC-PBG-(A&B).

($C_i = 20$ ppm, adsorbent dose = 10.0 mg, volume of soln. = 10 mL, pH = 7, at room temperature).

The figure shows that the highest rate of removal of Lead ions Pb^{2+} was with NCC-PBG-A after 5.0 minutes of shaking, and this percentage is 93.8%. Whereas, with NCC-PBG-B the removal percentage is 98.8% and the optimum contact time is after 10.0 minutes. We note that the removal rates of Lead ions Pb^{2+} by NCC-PBG-B are close in value with a percentage of 97.9% after one minute. This is close to the removal rate at the optimum contact time, so that much time can be saved when using this polymer.

For both polymers, the residual concentration of Pb^{2+} ions after the optimum contact time becomes almost constant. The extremely high rates of Lead ions Pb^{2+} removal is due to the very large availability of vacant sites on the outer surface of the adsorbent.

Based on that, we note that NCC-PBG-B is better than NCC-PBG-A because it removes a higher percentage of Lead ions Pb^{2+} with less contact time.

3.4.2.2 Effect of pH value

Figure 3.10 represents the effect of the pH on the removal efficiency of Pb^{2+} ions on the different polymers. These studies were conducted at the optimal contact times for NCC-PBG-A and NCC-PBG-B, while changing the pH value of the solution.

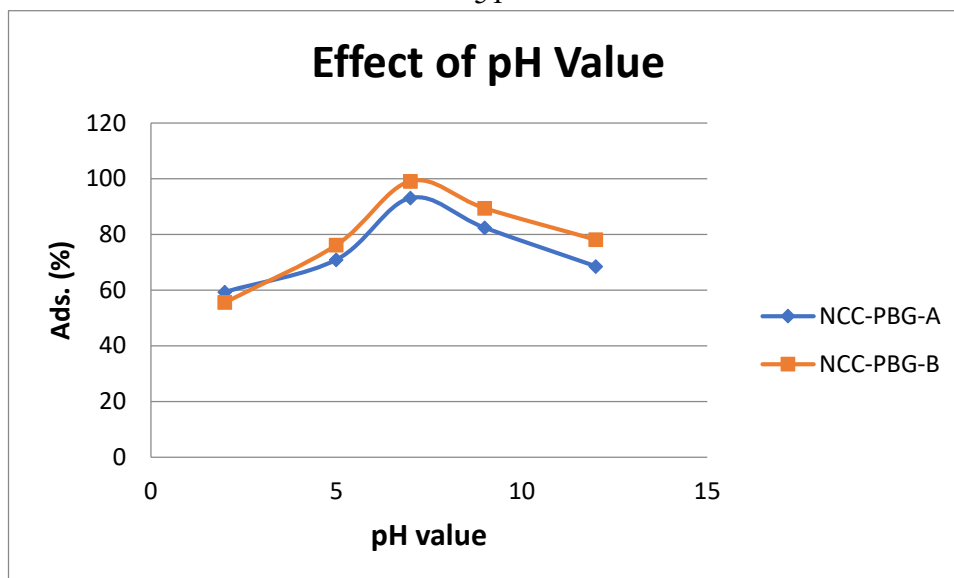


Figure 3.10: Effect of pH value on the adsorption of Pb^{2+} on NCC-PBG-(A&B) ($C_i = 20.0$ ppm, adsorbent dose = 0.01 g, volume of soln. = 10.0 mL, for 5.0 min, at room temperature).

For the NCC-PBG-A polymer, as previously observed with Copper ions Cu^{2+} , we note that the rate of Lead ions Pb^{2+} extraction increases with increasing the pH until a maximum at pH 7.0 is reached, and then it decreases with further increase in pH. This polymer had a maximum removal for Pb^{2+} of 93.1% compared to NCC-PBG-B which had a maximum removal of 99.1%.

As previously mentioned, the increase in the rate of metal ions removal with the increase in pH is due to the lack of competition between the protons and the positive metal ions on the vacant binding sites on the surface of the polymer itself and also due to the decrease in the positive surface charge, which leads to an increase in the metal ions bonding, as the electrostatic repulsion between surface polymer adsorbent and Lead ions Pb^{2+} . Whereas,

the decreasing behavior of the Pb^{2+} removal ratio after the optimum pH for both polymers may be due to the formation of soluble hydroxy complexes, which reduces the adsorption efficiency of removing Lead ions Pb^{2+} from the solution.

3.4.2.3 Effect of Temperature

To determine the effect of temperature on the adsorption of Lead ions Pb^{2+} using NCC-PBG-A or NCC-PBG-B, optimum conditions for contact time and pH were considered. In general, the adsorption efficiency becomes very low at high temperatures.

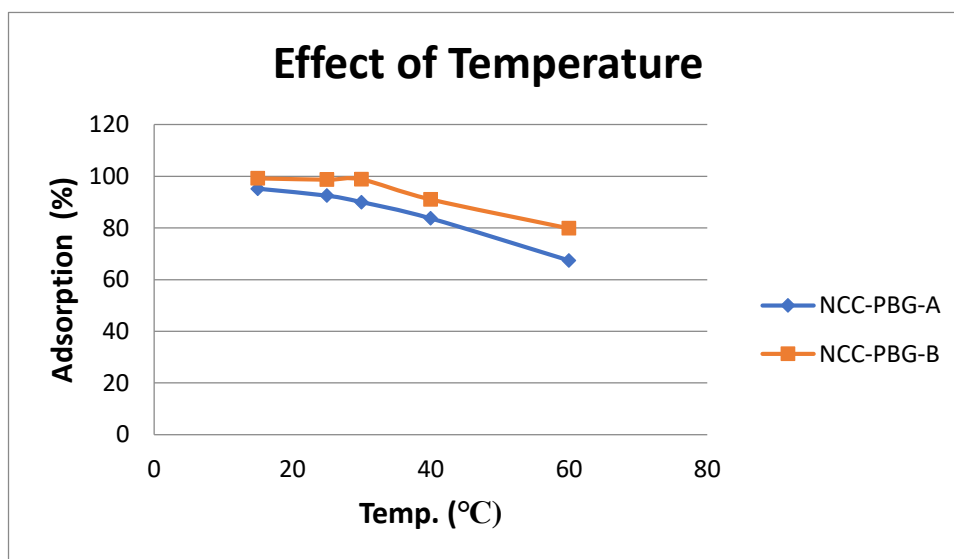


Figure 3.11: Effect of temperature on the adsorption of Pb^{2+} on NCC-PBG-(A&B) ($C_i = 20.0$ ppm, adsorbent dose = 10.0 mg, volume of soln. = 10.0 mL, for 5.0 min, pH = 7.0).

As shown in Figure 3.11, Lead ions Pb^{2+} are adsorbed with the modified cellulose polymers (NCC-PBG-A and NCC-PBG-B). The rate of Lead ion Pb^{2+} removal decreases at higher temperatures. Removal of lead ions reached

95.2% for NCC-PBG-A polymer at a temperature of 15.0°C. It was considered the optimum temperature for removing Lead ions Pb^{2+} by this polymer. The removal of Lead ions reached 99.2% when using NCC-PBG-B polymer at the same temperature. However, high removal rates can be achieved at room temperature as well, without the need to cool or heat the solution.

In general, the lower temperatures of the solution enhance the bonding ability between Lead ions Pb^{2+} and both polymers.

3.4.2.4 Effect of Adsorbent Dosage

The experimental results of lead ions stripping by modified cellulose polymers with respect to each dose of adsorbents are shown in figure 3.12 over a range of 5.0 mg to 100.0 mg at optimal values of contact time, pH and temperature.

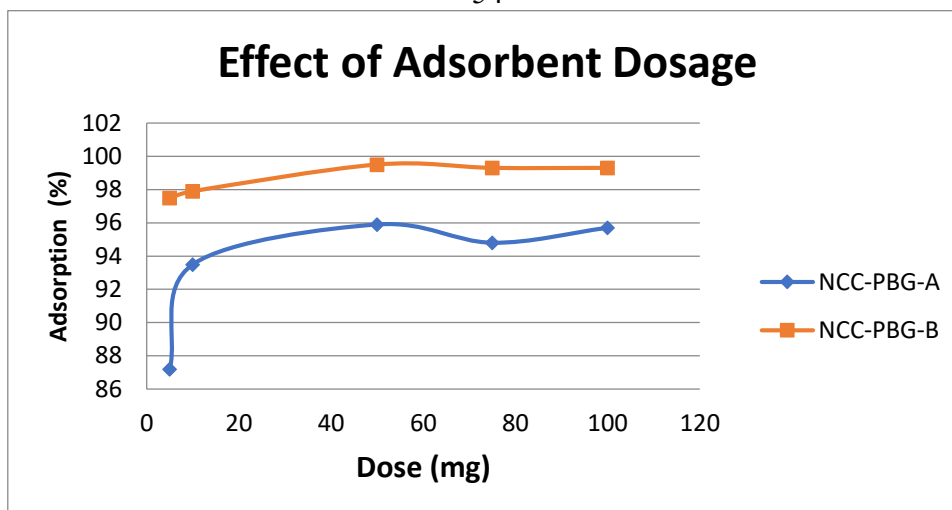


Figure 3.12: Effect of adsorbent dosage on the adsorption of Pb^{2+} on NCC-PBG-(A&B)

($C_i = 20.0$ ppm, volume of soln. = 10.0 mL, for 5.0 min , pH = 7.0 & 25°C).

The graph shows that the maximum rate of removal of Lead ions Pb^{2+} is reached with 50.0 mg of NCC-PBG-A. This polymer showed an increase in the percentage removal with an increase in the adsorbent dose. The same behavior of NCC-PBG-B at 50.0 mg dose was also observed.

And previously noted with Copper ions Cu^{2+} , the adsorption rate increases with the increase in the dose of the adsorbent and this is very intuitive and logical, because increasing the dose increases the vacant sites for metal ions binding on the surface of the adsorbent material, but the adsorption rates are high relatively even at small doses. The effect of dose control is expected to appear when the quantity of the solution changes and not the concentration of metal ions in the solution. This may explain the large abundance of vacant sites on the surface of the adsorbent material even when small doses of the adsorbent polymer are used.

3.4.2.5 Effect of Lead ions (Pb^{2+}) Initial Concentration

Figure 3.13 shows the effect of the concentration of Lead ions Pb^{2+} on the percentage of removal of these ions on both polymers. The graph shows that the adsorption rate increases with increasing the concentration of lead ions Pb^{2+} .

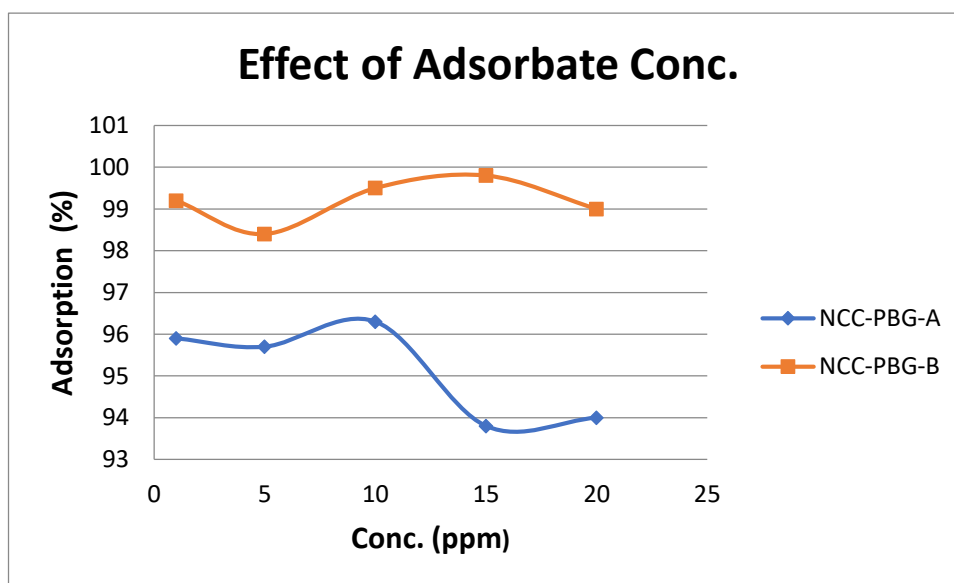


Figure 3.13: Effect of adsorbent dosage on the adsorption of Pb^{2+} on NCC-PBG-(A&B)

(adsorbent dose = 10.0 mg , volume of soln. = 10.0 mL , for 5.0 min , pH = 7.0 , at room temperature).

The maximum percentage of these ions is 99.8% for NCC-PBG-B using 15.0 ppm of Lead Pb^{2+} , while the optimum concentration of Lead ions Pb^{2+} was 10.0 ppm for NCC-PBG-A, and this explains the limited binding sites on the surface of this polymer.

The following table (3.2) represents the adsorption results for removing Lead ions Pb^{2+} from solution using NCC-PBG-A or NCC-PBG-B adsorbents.

Table 3.2: The adsorption results for removing Pb^{2+} from soln. using NCC-PBP-(A & B)

Adsorption of Pb^{2+}		
Optimum Condition and % of Pb^{2+} Adsorption	NCC-PBG-A	NCC-PBG-B
Contact Time (minute)	5.0	10.0
% of Adsorption	93.8%	98.8%
pH value	7.0	7.0
% of Adsorption	93.1%	99.1%
Temperature ($^{\circ}C$)	15.0	15.0
% of Adsorption	95.2%	99.2%
Adsorbent Dose (mg)	50.0	50.0
% of Adsorption	95.9%	99.5%
Adsorbate Concentration(ppm)	10.0	15.0
% of Adsorption	96.3%	99.8%

3.5 Adsorption Kinetics

In order to explain the mechanism by which metal ions are adsorbed, the results must be studied based on the laws of kinetics.

Two models were used to describe adsorption kinetics: pseudo-first order (Eq. 6) and pseudo-second order (Eq. 7):

$$\ln(q_e - q_t) = \ln q_e - K_1 t \quad \text{Eq. 6}$$

$$\frac{t}{q_t} = \frac{1}{k_2 q_e^2} + \frac{t}{q_e} \quad \text{Eq. 7}$$

Where;

q_e : the mass of adsorbate/unit mass of adsorbent at equilibrium (mg/g)

q_t : the mass adsorbate/unit mass of adsorbent at time t (mg/g)

K_1 : the first-rate constant (min^{-1})

K_2 : the second-order rate constant ($\text{g mg}^{-1} \text{min}^{-1}$)

3.5.1 Adsorption of Cu^{2+} Ions

3.5.1.1 Testing the two models on NCC-PBG-A

The results for fitting the adsorption data for Cu^{2+} ions on NCC-PBG-A to pseudo-first order and pseudo-second order laws are shown in the following tables (3.3) and figure (3.14).

Table 3.3: Pseudo-first order model for the adsorption of Cu^{2+} on NCC-PBG-A

Time (min)	Conc. of Cu^{2+} after removal	q_t (mg/g)	$\ln(q_e - q_t)$
1.0	12.8241	7.1759	1.779028777
5.0	9.4428	10.5572	0.933265836
10.0	6.9838	13.0162	-2.479322271
15.0	6.9175	13.0825	-4.045554398
20.0	7.0273	12.9727	-2.061208773

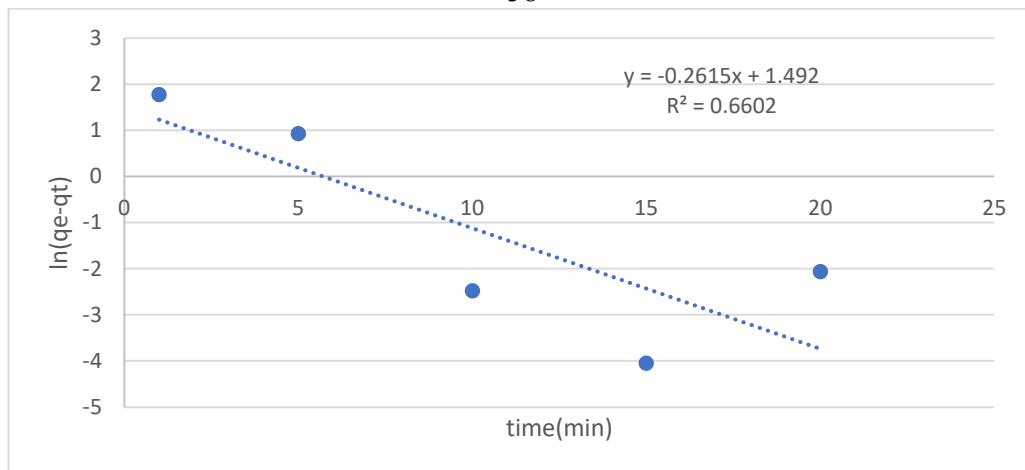


Fig. 3.14: Pseudo-first order model for the adsorption of Cu^{2+} on NCC-PBG-A

Table 3.4: Pseudo-second order model for the adsorption of Cu^{2+} on NCC-PBG-A

Time (min)	Conc. of Cu^{2+} after removal	q_t (mg/g)	$\frac{t}{q_t}$
1.0	12.8241	7.1759	0.139355
5.0	9.4428	10.5572	0.47361
10.0	6.9838	13.0162	0.768273
15.0	6.9175	13.0825	1.14657
20.0	7.0273	12.9727	1.541699

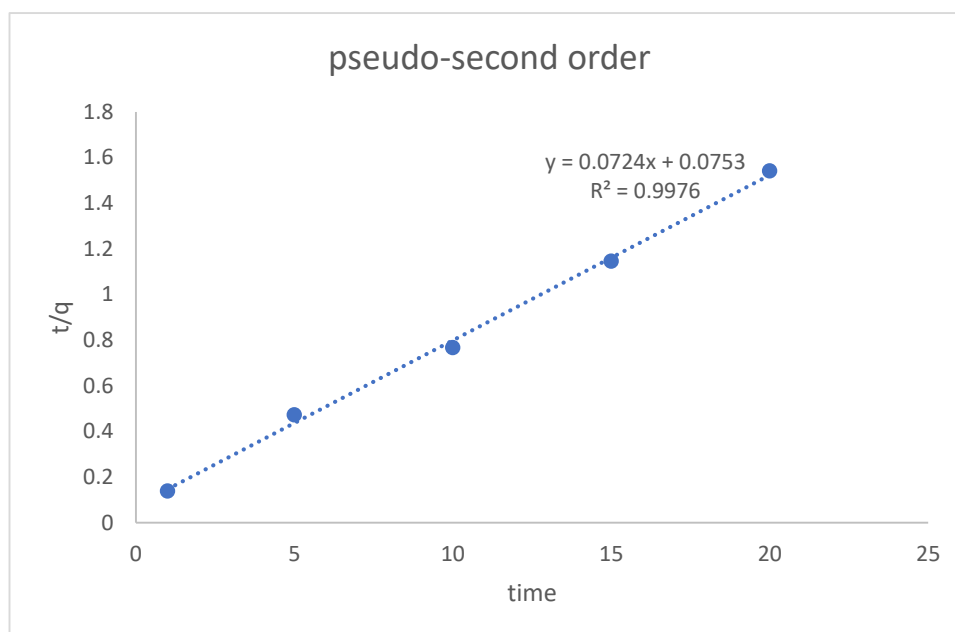


Fig. 3.15: Pseudo-second order model for the adsorption of Cu^{2+} on NCC-PBG-A

3.5.1.2 Testing the two models on NCC-PBG-B

The results for fitting the adsorption data for Cu^{2+} ions on NCC-PBG-B to pseudo-first order and pseudo-second order laws are shown in the following tables and figures.

Table 3.5: Pseudo-first order model for the adsorption of Cu^{2+} on NCC-PBG-B

Time (min)	Conc. of Cu^{2+} after removal	q_t (mg/g)	$\ln(q_e - q_t)$
1.0	7.7959	12.2041	1.807616414
5.0	3.5598	16.4402	0.620468955
10.0	1.8037	18.1963	-2.266253164
15.0	1.761	18.239	-2.796881415
20.0	1.7909	18.2091	-2.397995278

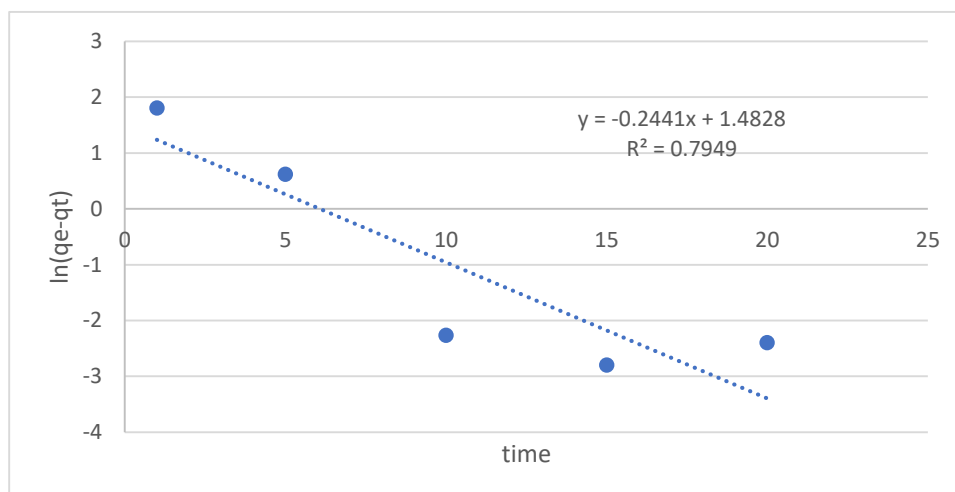


Fig. 3.16: Pseudo-first order model for the adsorption of Cu^{2+} on NCC-PBG-B

Table 3.6: Pseudo-second order model for the adsorption of Cu^{2+} on NCC-PBG-B

Time (min)	Conc. of Cu^{2+} after removal	q_t (mg/g)	$\frac{t}{q_t}$
1.0	7.7959	12.2041	0.08193968
5.0	3.5598	16.4402	0.30413255
10.0	1.8037	18.1963	0.54956227
15.0	1.761	18.239	0.82241351
20.0	1.7909	18.2091	1.09835192

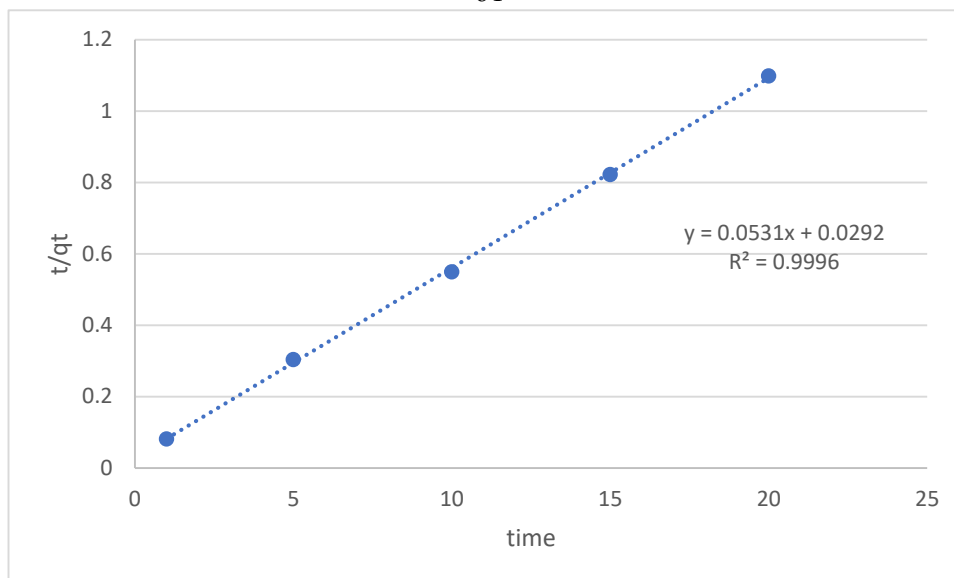


Fig. 3.17: Pseudo-second order model for the adsorption of Cu^{2+} on NCC-PBG-B

3.5.2 Adsorption of Pb^{2+} Ions

3.5.2.1 Testing the two models on NCC-PBG-A

The results for fitting the adsorption data for Pb^{2+} ions on NCC-PBG-A to pseudo-first order and pseudo-second order laws are shown in the following tables and figures.

Table 3.7: Pseudo-first order model for the adsorption of Pb^{2+} on NCC-PBG-A

Time (min)	Conc. of Pb^{2+} after removal	q_t (mg/g)	$\ln(q_e - q_t)$
1.0	4.3228	15.6772	1.13873004
5.0	1.2419	18.7581	-3.1724695
10.0	1.5213	18.4787	-1.13538
15.0	1.8604	18.1396	-0.4149096
20.0	2.0795	17.9205	-0.1284017

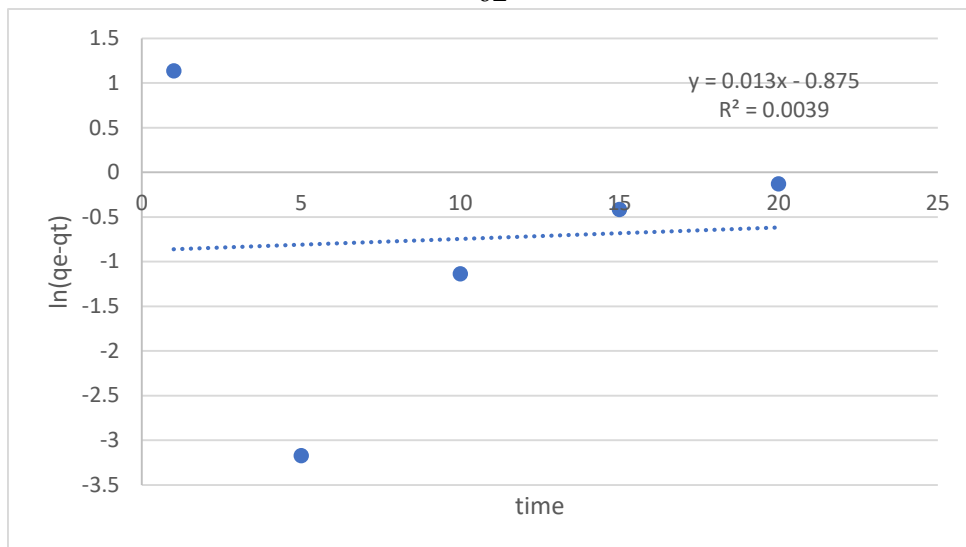


Fig.3.18: Pseudo-first order model for the adsorption of Pb^{2+} on NCC-PBG-A

Table 3.8: Pseudo-second order model for the adsorption of Pb^{2+} on NCC-PBG-A

Time (min)	Conc. of Pb^{2+} after removal	q_t (mg/g)	$\frac{t}{q_t}$
1.0	4.3228	15.6772	0.0637869
5.0	1.2419	18.7581	0.26655152
10.0	1.5213	18.4787	0.54116361
15.0	1.8604	18.1396	0.82692011
20.0	2.0795	17.9205	1.11604029

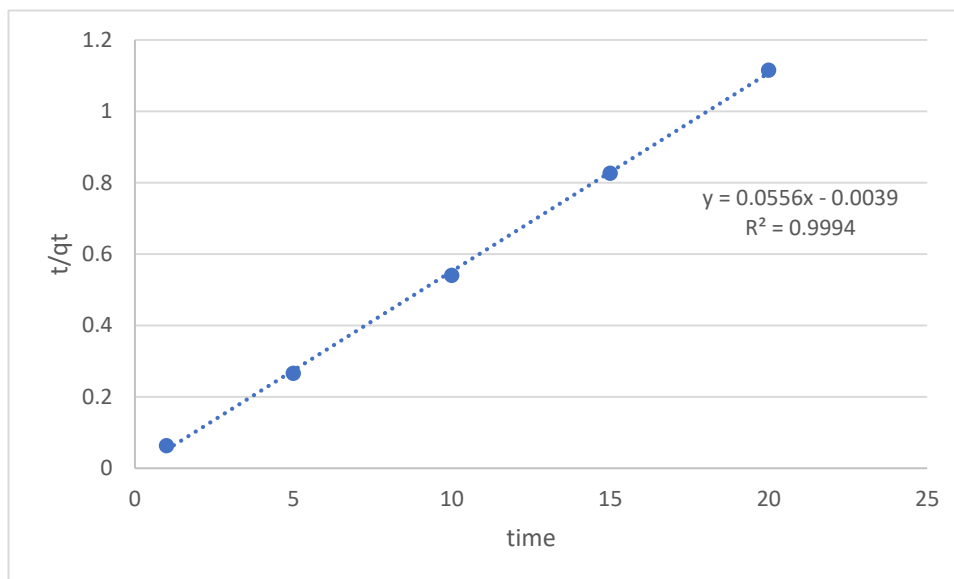


Fig. 3.19: Pseudo-second order model for the adsorption of Pb^{2+} on NCC-PBG-A

3.5.2.2 Testing the two models on NCC-PBG-B

The results for fitting the adsorption data for Pb^{2+} ions on NCC-PBG-B to pseudo-first order and pseudo-second order laws are shown in the following tables and figures.

Table 3.9: Pseudo-first order model for the adsorption of Pb^{2+} on NCC-PBG-B

Time (min)	Conc. of Pb^{2+} after removal	q_t (mg/g)	$\ln(q_e - q_t)$
1.0	0.4218	19.5782	-1.5059792
5.0	0.4971	19.5029	-1.2136865
10.0	0.2399	19.7601	-3.221379
15.0	0.3605	19.6395	-1.8294613
20.0	0.3593	19.6407	-1.8369661

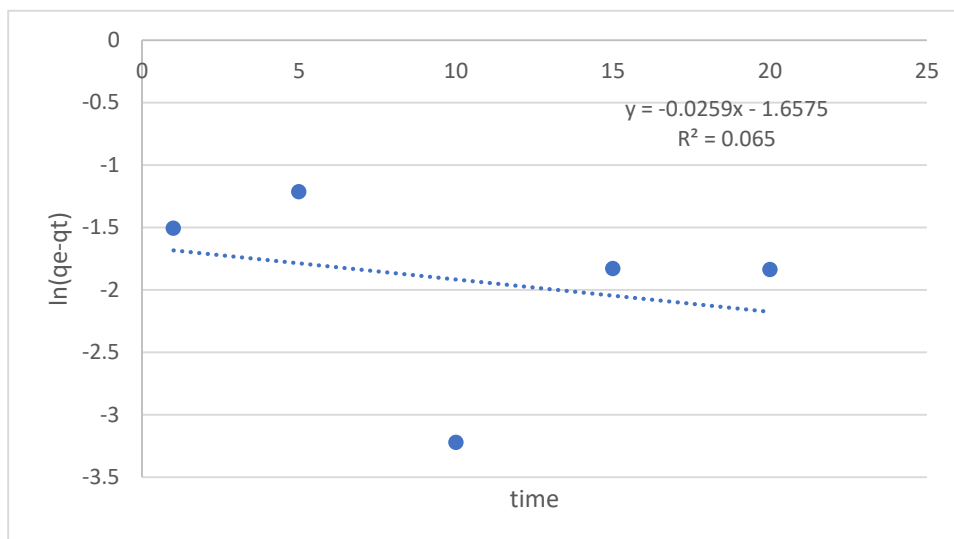


Fig.3.20: Pseudo-first order model for the adsorption of Pb^{2+} on NCC-PBG-B

Table 3.10: Pseudo-second order model for the adsorption of Pb^{2+} on NCC-PBG-B

Time (min)	Conc. of Pb^{2+} after removal	q_t (mg/g)	$\frac{t}{q_t}$
1.0	0.4218	19.5782	0.0510772
5.0	0.4971	19.5029	0.2563721
10.0	0.2399	19.7601	0.5060703
15.0	0.3605	19.6395	0.7637669
20.0	0.3593	19.6407	1.0182936

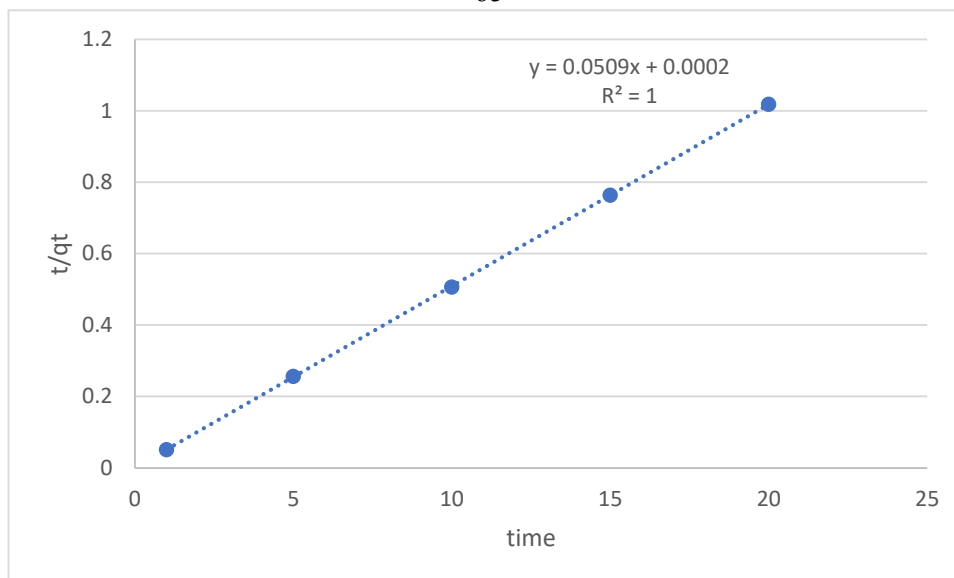


Fig.3.21: Pseudo-second order model for the adsorption of Pb^{2+} on NCC-PBG-B

Table 3.11: Summary of adsorption kinetic

	Adsorption kinetic							
	Copper ion (Cu^{2+})				Lead ion (Pb^{2+})			
	NCC-PBG-A		NCC-PBG-B		NCC-PBG-A		NCC-PBG-B	
	First order	Second order	First order	Second order	First order	Second order	First order	Second order
R^2	0.660	0.997	0.794	0.999	0.003	0.999	0.06	1
Theo. q_e	13.1	13.1	18.3	18.3	18.8	18.8	19.8	19.8
Exp. q_e	4.446	13.8	4.405	18.83	0.417	17.98	0.191	19.65
K_1	0.2615	-	0.2441	-	-0.013	-	0.026	-
K_2	-	0.0697	-	0.0965	-	-0.793	-	12.95

As shown in table 3.11, the obtained correlation coefficients (R^2) for the pseudo-second order were higher than for the pseudo-first order in all cases. For example, when applying the results to the pseudo-first-order equation for

NCC-PBG-A with Copper ions Cu^{2+} the value of R^2 was 0.66, and when applying to the pseudo-second-order equation, the value of R^2 was 0.997, and the calculated q_e values were 13.1 mg/g, 18.3 mg/g, 18.8 mg/g and 19.8 mg/g. The experimental values for q_e values were 13.8 mg/g, 18.83 mg/g, 17.98 mg/g and 19.65 mg/g.

The experimental and theoretical results are in a good agreement, indicating that the adsorption process of Copper ions Cu^{2+} and Lead ions Pb^{2+} on the surfaces of NCC-PBG-(A & B) polymers follows a pseudo-second order model.

3.6 Adsorption Isotherms

Langmuir (Eq. 8) and Freundlich (Eq. 9) isotherms were applied to study the efficiency of the polymers that were prepared in removing both Copper Cu^{2+} and Lead Pb^{2+} ions at equilibrium.

If the ions are arranged in a single layer on the surface of the polymer, the adsorption process follows the Langmuir model. Whereas, if the adsorption process between the ions and the polymer surface is carried out on several heterogeneous layers, the process follows the Freundlich model.

$$\frac{1}{q_e} = \frac{1}{Q_{\max} K_L C_e} + \frac{1}{Q_{\max}} \quad (\text{Eq. 8})$$

Where; C_e : the equilibrium conc. of ions (ppm).

q_e : the mass of adsorbate adsorbed per unit mass of polymer at equilibrium (mg/g).

Q_{\max} : the monolayer adsorption capacity of the adsorbent (mg/g) theoretically.

K_l : the Langmuir affinity constant related to the adsorption energy (L/mg).

$$\ln q_e = \ln k_f + \frac{1}{n} \ln C_e \quad (\text{Eq. 9})$$

Where;

K_f : the Freundlich constant related to adsorption capacity (mg/g).

n : the heterogeneity coefficient (g/L).

Langmuir's equation can be used to determine whether or not the adsorption process is attractive and appropriate using the R_l constant

(Eq. 9) derived from the Langmuir model.

$$R_l = \frac{1}{1 + K_l C_i} = 1 + \frac{1}{K_l C_i} \quad (\text{Eq. 9})$$

Where;

C_i : the initial adsorbate conc. (ppm).

R_l : the dimensionless constant separation factor.

$$\text{If } \left\{ \begin{array}{ll} R_l > 1 & : \text{ adsorption is unfavourable} \\ 1 > R_l > 0 & : \text{ adsorption is favourable} \\ R_l = 1 & : \text{ adsorption is linear} \end{array} \right\}$$

3.6.1 Adsorption of Cu^{2+}

3.6.1.1 Testing the two models on NCC-PBG-A

The data for the adsorption of Cu^{2+} on NCC-PBG-A were applied to the two isotherms. The results are shown in tables (3.12, 3.13) and figures (3.22, 3.23).

Table 3.12: Langmuir model for adsorption of Cu^{2+} on NCC-PBG-A

Conc. of copper ions before removal (ppm)	Conc. of Cu^{2+} after removal	q_e	$\frac{1}{C_e}$	$\frac{1}{q_e}$
1.0	0.231	0.769	4.32900433	1.30039012
5.0	1.4599	3.5401	0.68497842	0.2824779
10.0	2.7897	7.2103	0.35846148	0.13869048
15.0	4.545	10.455	0.220022	0.09564802
20.0	6.8978	13.1022	0.14497376	0.07632306

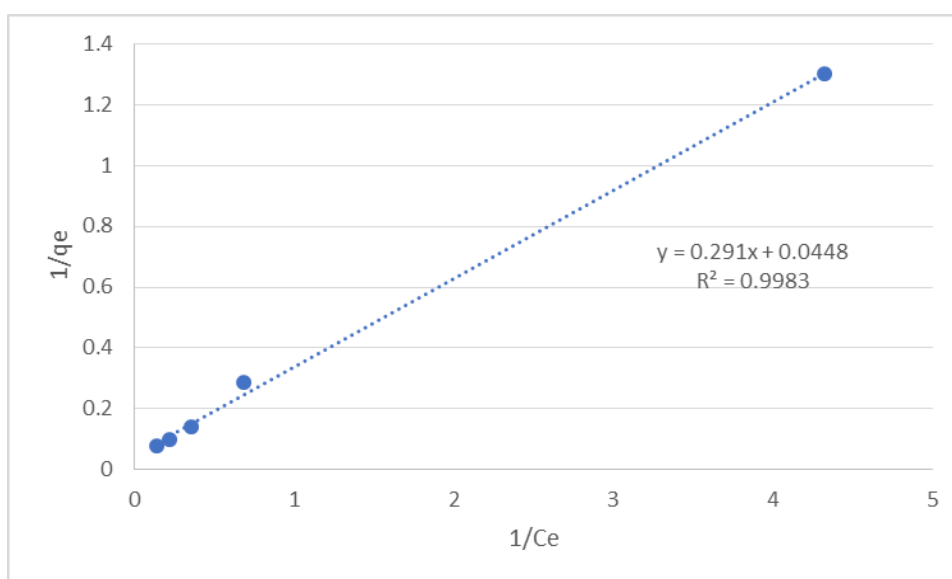
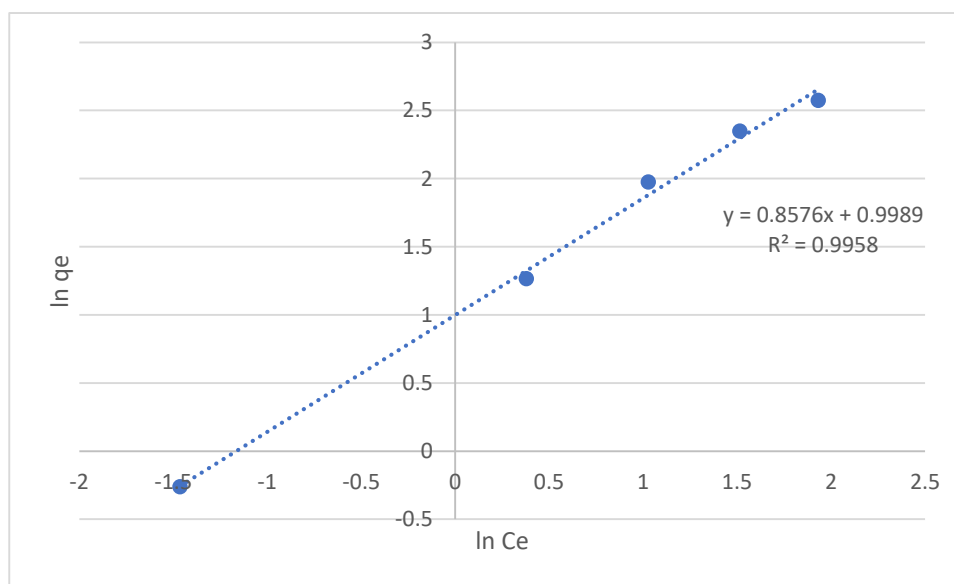


Figure 3.22: Langmuir model for adsorption of Cu^{2+} on NCC-PBG-A

Table 3.13: Freundlich model for adsorption of Cu^{2+} on NCC-PBG-A

Conc. of copper ions before removal (ppm)	Conc. of Cu^{2+} after removal	C_e	$\ln C_e$	$\ln q_e$
1.0	0.231	0.769	-1.465337568	-0.2626643
5.0	1.4599	3.5401	0.37836794	1.26415498
10.0	2.7897	7.2103	1.025934063	1.97551056
15.0	4.545	10.455	1.514027728	2.34708033
20.0	6.8978	13.1022	1.93120252	2.57278016

**Fig. 3.23: Freundlich model for adsorption of Cu^{2+} on NCC-PBG-A**

3.6.1.2 Testing the two models on NCC-PBG-B

The data for the adsorption of Cu^{2+} ions on NCC-PBG-B were applied to the two isotherms. The results are shown in tables (3.14, 3.15) and figures (3.24, 3.25).

Table 3.14: Langmuir model for adsorption of Cu^{2+} on NCC-PBG-B

Conc. of Copper ions before removal (ppm)	Conc. of Cu^{2+} after removal	q_e	$\frac{1}{C_e}$	$\frac{1}{q_e}$
1.0	0.043	0.957	23.255814	1.04493208
5.0	0.1115	4.8885	8.96860987	0.20456173
10.0	0.8207	9.1793	1.21847204	0.10894077
15.0	1.0498	13.9502	0.95256239	0.07168356
20.0	1.7053	18.2947	0.58640708	0.05466064

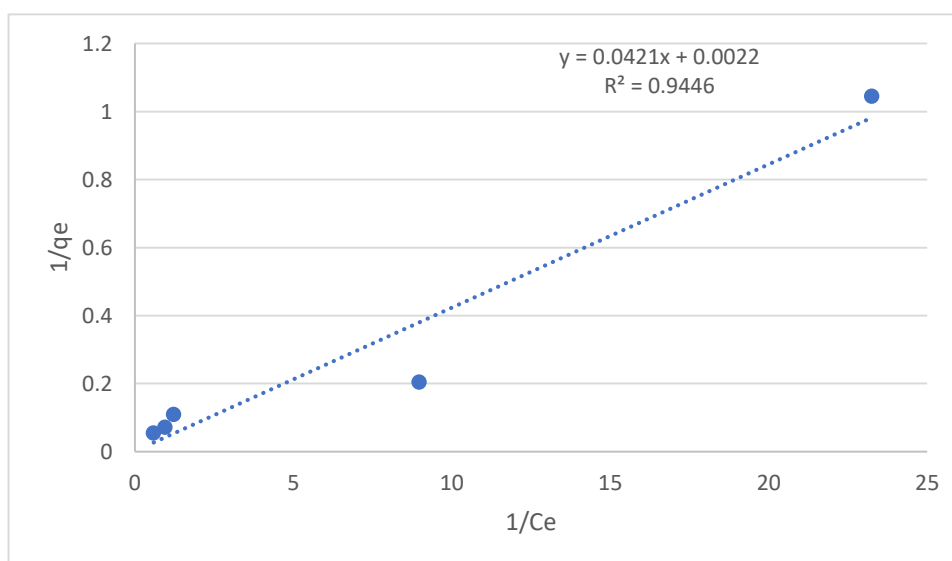
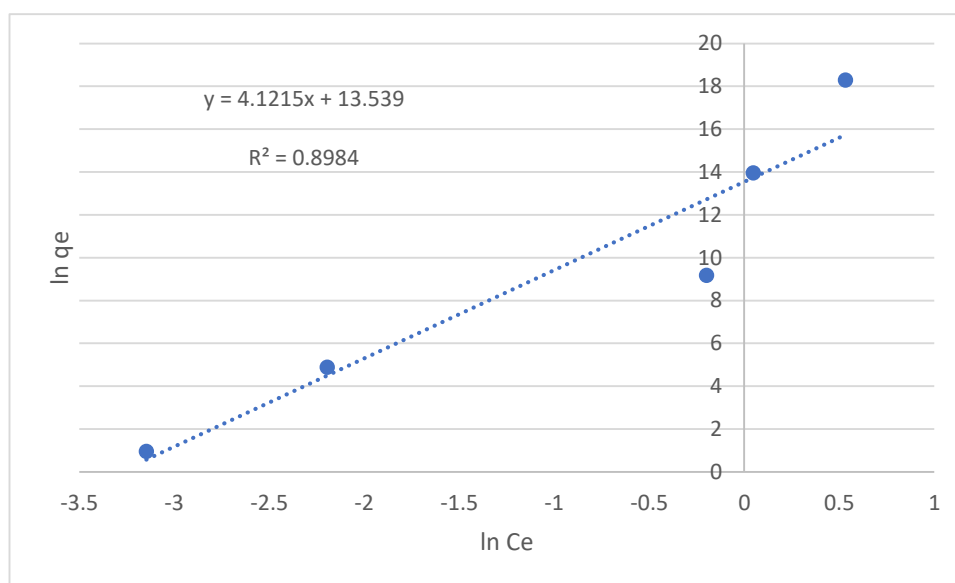


Fig. 3.24: Langmuir model for adsorption of Cu^{2+} on NCC-PBG-B

Table 3.15: Freundlich model for adsorption of Cu^{2+} on NCC-PBG-B

Conc. of copper ions before removal (ppm)	Conc. of Cu^{2+} after removal	C_e	$\ln C_e$	$\ln q_e$
1.0	0.043	0.957	-	0.957
5.0	0.1115	4.8885	-	4.8885
10.0	0.8207	9.1793	-	9.1793
15.0	1.0498	13.9502	0.04859967	13.9502
20.0	1.7053	18.2947	0.533741048	18.2947

Fig. 3.25: Freundlich model for adsorption of Cu^{2+} on NCC-PBG-B

3.6.2 Adsorption of Pb^{2+}

3.6.2.1 Testing the two models on NCC-PBG-A

The data for the adsorption of Pb^{2+} ions on NCC-PBG-A were applied to the two isotherms. The results are shown in tables (3.16, 3.17) and figures (3.26, 3.27).

Table 3.16: Langmuir model for adsorption of Pb^{2+} on NCC-PBG-A

Conc. of lead ions before removal	Conc. of Pb^{2+} after	q_e	$\frac{1}{C_e}$	$\frac{1}{q_e}$
1.0	0.0413	0.9587	24.2130751	1.0430792
5.0	0.2149	4.7851	4.65332713	0.208982
10.0	0.3697	9.6303	2.70489586	0.1038389
15.0	0.9308	14.0692	1.07434465	0.0710772
20.0	1.2002	18.7998	0.83319447	0.0531921

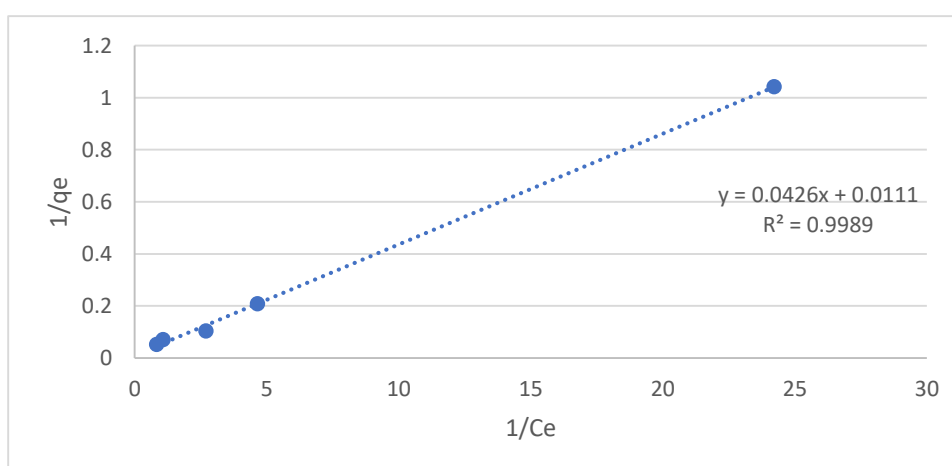
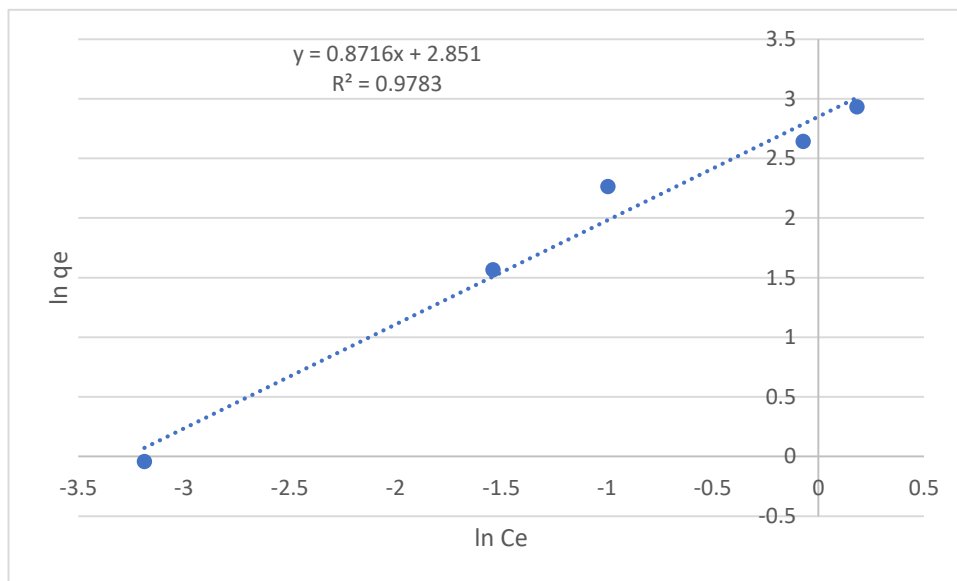


Fig. 3.26: Langmuir model for adsorption of Pb^{2+} on NCC-PBG-A

Table 3.17: Freundlich model for adsorption of Pb^{2+} on NCC-PBG-A

Conc. of lead ions before removal (ppm)	Conc. of Pb^{2+} after removal	C_e	$\ln C_e$	$\ln q_e$
1.0	0.0413	0.9587	-3.18689278	-0.04218
5.0	0.2149	4.7851	-1.53758248	1.565507
10.0	0.3697	9.6303	-0.99506341	2.264914
15.0	0.9308	14.0692	-0.07171085	2.643988
20.0	1.2002	18.7998	0.18248821	2.933846

Fig. 3.27: Freundlich model for adsorption of Pb^{2+} on NCC-PBG-A

3.6.2.2 Testing the two models on NCC-PBG-B

The data for the adsorption of Pb^{2+} on NCC-PBG-B were applied to the two isotherms. The results are shown in tables (3.18, 3.19) and figures (3.28, 3.29).

Table 3.18: Langmuir model for adsorption of Pb^{2+} on NCC-PBG-B

Conc. of lead ions before removal (ppm)	Conc. of Pb^{2+} after removal	q_e	$\frac{1}{C_e}$	$\frac{1}{q_e}$
1.0	0.008	0.992	125	1.00806452
5.0	0.0805	4.9195	12.4224	0.20327269
10.0	0.0513	9.9487	19.4932	0.10051565
15.0	0.0302	14.9698	33.1126	0.06680116
20.0	0.1994	19.8006	5.01505	0.05050352

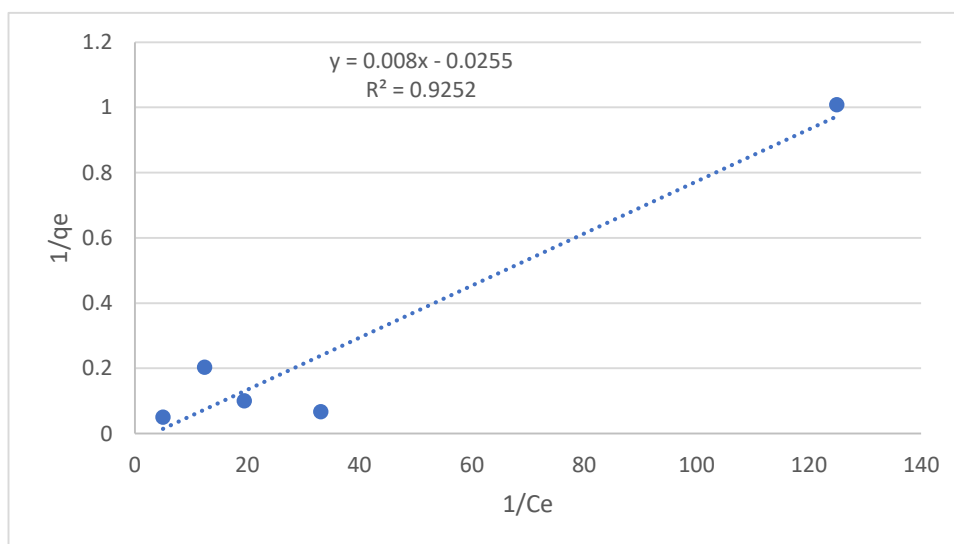
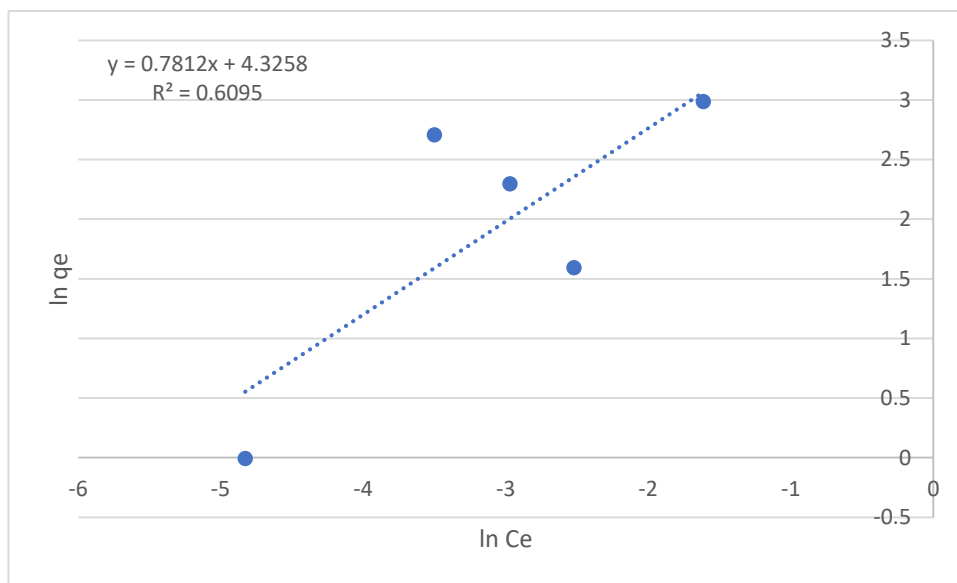


Fig. 3.28: Langmuir model for adsorption of Pb^{2+} on NCC-PBG-B

Table 3.19: Freundlich model for adsorption of Pb^{2+} on NCC-PBG-B

Conc. of lead ions before removal (ppm)	Conc. of Pb^{2+} after removal	C_e	$\ln C_e$	$\ln q_e$
1.0	0.008	0.992	-4.82831	-0.0080322
5.0	0.0805	4.9195	-2.5195	1.5932069
10.0	0.0513	9.9487	-2.97006	2.2974419
15.0	0.0302	14.969	-3.49991	2.7060348
20.0	0.1994	19.800	-1.61244	2.9857122

**Fig. 3.29:** Freundlich model for adsorption of Pb^{2+} on NCC-PBG-B

The following table (3.20) represents the values of the Langmuir and Freundlich isothermal coefficients for adsorption of both Cu^{2+} and Pb^{2+} ions on the surface of the polymers NCC-PBG-A and NCC-PBG-B.

Table 3.20: Summary Adsorption Isotherms for NCC-PBG-(A & B)

Copper ion Cu^{2+}						
NCC-PBG-A						
Langmuir				<i>Freundlich</i>		
R^2	Q_{\max}	K_l	R_l	R^2	n	K_f
0.9983	22.321	0.153	0.245	0.9958	1.166	2.715
NCC-PBG-B						
Langmuir				<i>Freundlich</i>		
R^2	Q_{\max}	K_l	R_l	R^2	n	K_f
0.9446	454.545	0.052	0.489	0.8984	0.243	758425.61

Lead ion Pb^{2+}						
NCC-PBG-A						
Langmuir				<i>Freundlich</i>		
R^2	Q_{\max}	K_l	R_l	R^2	n	K_f
0.9989	90.090	0.2605	0.161	0.9783	1.147	17.305
NCC-PBG-B						
Langmuir				<i>Freundlich</i>		
R^2	Q_{\max}	K_l	R_l	R^2	n	K_f
0.9252	39.216	3.188	0.0154	0.6095	1.2801	75.626

We note that R^2 values with Langmuir isotherm in all cases are very close to 1. This means that the adsorption of both Copper Cu^{2+} and Lead Pb^{2+} ions on

the surface of the polymers (NCC-PBG-A and NCC-PBG-B) follow the Langmuir isotherm.

3.7 Adsorption Thermodynamics

Using the thermodynamic equation of the Van't Hoff plot. The thermodynamic parameters (ΔH and ΔS) of the absorption of copper ions Cu^{2+} on (NCC-PBG-A) or (NCC-PBG-B) can be calculated from the slope and y-intercept of the graph of $\ln K_d$ versus $(\frac{1}{T})$.

3.7.1 Adsorption of Cu^{2+}

3.7.1.1 Testing the Thermodynamic equation on NCC-PBG-A

The data for the adsorption of Cu^{2+} on NCC-PBG-A were applied to the thermodynamic. The results are shown in table (3.21) and figure (3.30).

Table 3.21: Adsorption of Cu^{2+} on **NCC-PBG-A**

Temp.	C_e	$1/T$ (K^{-1})	$\ln K_d$
15	6.8015	0.003472	0.66296
25	6.2403	0.003356	0.790716
30	7.7396	0.0033	0.460025
40	11.8599	0.003195	-0.37636
60	14.8203	0.003003	-1.05125

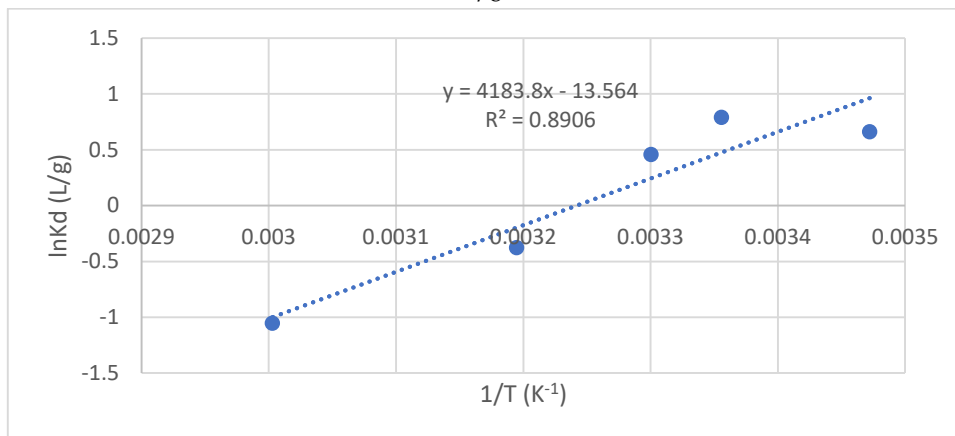


Fig. 3.30: Van't Hoff plot for the adsorption of Cu^{2+} on NCC-PBG-A (time = 10 minute, $C_i = 20.0$ ppm, pH = 7.0, adsorbent dose = 10.0 mg, volume = 10.0 mL).

3.7.1.2 Testing the Thermodynamic equation on NCC-PBG-B

The data for the adsorption of Cu^{2+} on NCC-PBG-B were applied to the thermodynamic equation. The results are shown in table (3.22) and figure (3.31).

Table 3.22: Thermodynamic results for adsorption of Cu^{2+} on NCC-PBG-B

Temp.	C_e	1/T (K ⁻¹)	lnK _d
15	3.22	0.003472	1.650806
25	1.52	0.003356	2.497979
30	5.04	0.0033	1.087974
40	8.26	0.003195	0.351577
60	13.36	0.003003	-0.69915

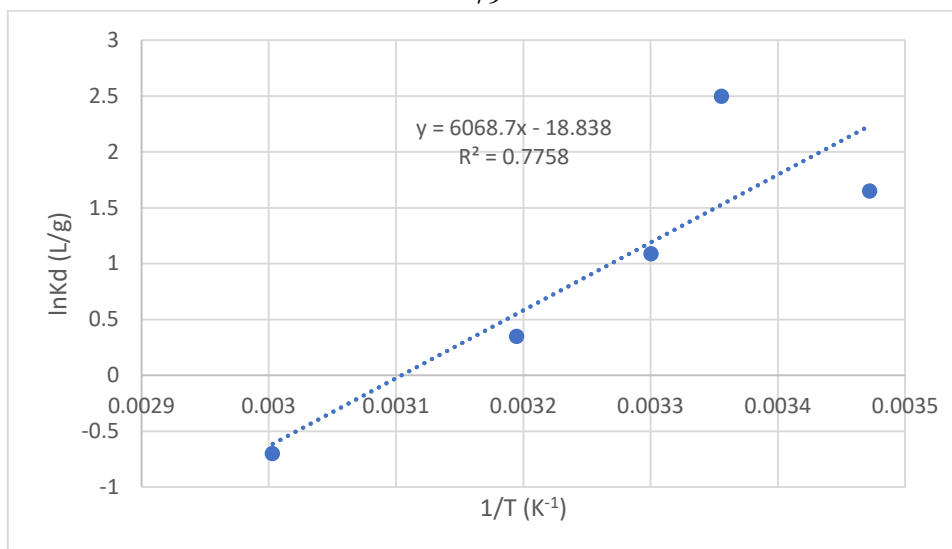


Figure 3.31: Van't Hoff plot for the adsorption of Cu^{2+} on NCC-PBG-B (time = 10.0 minute, $C_i = 20.0$ ppm, pH = 7.0, adsorbent dose = 10.0 mg, volume = 10.0 mL).

The following table represents the values of the thermodynamic parameters ΔS and ΔH for the adsorption of Cu^{2+} on NCC-PBG-(A & B).

Table 3.23: The thermodynamic parameters for the adsorption of Cu^{2+} on NCC-PBG-(A & B)

Adsorbents	Adsorption of Cu^{2+}	
	Adsorption Thermodynamics	
	ΔH (kJ)	ΔS (J/K)
NCC-PBG-A	-34.7775	-112.771
NCC-PBG-B	-50.4494	-156.619

As shown in this table, the adsorption of Cu^{2+} on NCC-PBG-A and NCC-PBG-B adsorbent is exothermic process ($\Delta H < 0$) and non-spontaneous ($\Delta S < 0$).

3.7.2 Adsorption of Pb^{2+}

3.7.2.1 Testing the Thermodynamic equation on NCC-PBG-A

The data for the adsorption of Pb^{2+} ions on NCC-PBG-A were applied to the thermodynamic equation. The results are shown in tables (3.24) and figures (3.32).

Table 3.24: Thermodynamic results for adsorption of Pb^{2+} on NCC-PBG-A

Temp.	C_e	$1/T$ (K^{-1})	$\ln K_d$
15	0.9597	0.003472	2.987692
25	1.5004	0.003356	2.512017
30	2.0171	0.0033	2.18776
40	3.2598	0.003195	1.636147
60	6.5204	0.003003	0.726242

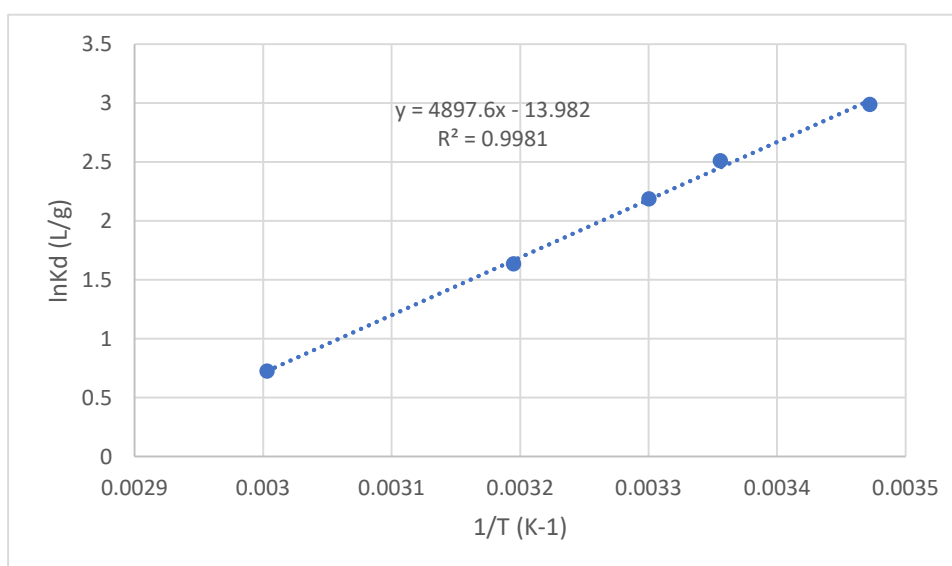


Figure 3.32: Van't Hoff plot for the adsorption of Pb^{2+} on NCC-PBG-A (time = 10.0 minute, C_i = 20.0 ppm, pH = 7.0, adsorbent dose = 10.0 mg, volume = 10.0 mL).

3.7.2.2 Testing the Thermodynamic equation on NCC-PBG-B

The data for the adsorption of Pb^{2+} on NCC-PBG-B were applied to the thermodynamic equation. The results are shown in tables (3.25) and figures (3.33).

Table 3.25: Thermodynamic results for adsorption of Pb^{2+} on NCC-PBG-B

Temp.	C_e	$1/T$ (K^{-1})	$\ln K_d$
15	0.1598	0.003472	4.821542
25	0.2599	0.003356	4.33011
30	0.2402	0.0033	4.409933
40	1.7798	0.003195	2.32603
60	4.0201	0.003003	1.380025

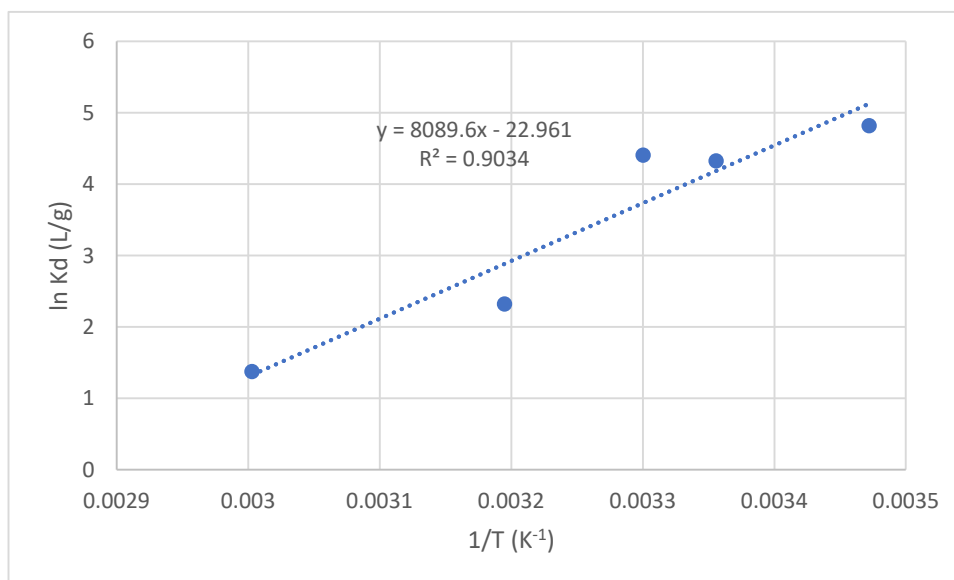


Figure 3.33: Van't Hoff plot for the adsorption of Pb^{2+} on NCC-PBG-B (time = 10.0 minute, $C_i = 20.0$ ppm, pH = 7.0, adsorbent dose = 10.0 mg, volume = 10.0 mL).

The following table represents the values of the thermodynamic parameters ΔS and ΔH for the adsorption of Pb^{2+} on NCC-PBG-(A&B).

Table 3.26: The thermodynamic parameters for the adsorption of Pb^{2+} on NCC-PBG-(A & B).

Adsorbents	Adsorption of Pb^{2+}	
	Adsorption Thermodynamics	
	ΔH (kJ)	ΔS (J/K)
NCC-PBG-A	-40.7186	-116.246
NCC-PBG-B	-67.2519	-190.898

As shown in this table, the adsorption of Pb^{2+} on NCC-PBG-A and NCC-PBG-B adsorbent is exothermic process ($\Delta H < 0$) and non spontaneous ($\Delta S < 0$).

3.8 Analysis for samples of sewage before & after the purification process

The efficiency of the modified nanocrystalline cellulose polymers (NCC-PBG-A and NCC-PBG-B) and their ability to adsorb toxic metal ions present in real wastewater from all human activities in homes, agriculture, or factories were studied at pH equals to 7.

Two samples of sewage water were prepared to be treated with the prepared polymers. Each sample was treated with a different polymer.

In both cases, we took into account the optimal conditions obtained in our study. We performed this assay at 25 ° C and a pH of 7 and 50 mg of polymer and shaken for 10 minutes.

The concentrations of the metal ions in each of the sewage samples before and after using the polymers are summarized in table (3.27). Metal ions concentrations were measured using ICP-MS. Excellent efficiency was achieved against all metal ions present in the wastewater samples.

Table 3.27: Results of the center of analyzes for the Conc. of toxic metals

Results of the center of analyzes for the Conc. of metal ions							
NCC-PBG-A				NCC-PBG-B			
Metal Ions	Conc. Before (ppb)	Conc. after (ppb)	Percentage Removals (%)	Metal Ions	Conc. Before (ppb)	Conc. after (ppb)	Percentage Removals (%)
Al	4680	25.898	99.4466239	Al	4680.0	16.058	99.6568803
Ag	38.2	0.867	97.7303665	Ag	38.2	0.873	97.7146597
Ga	2.4	0.327	86.375	Ga	2.4	0.083	96.5416667
Sr	609.0	99.055	83.7348112	Sr	609.0	84.201	86.1738916
Cs	0.31	0.056	81.9354839	Cd	0.31	0.051	83.5483871
Cr	523.0	19.516	96.2684512	Cr	523.0	21.268	95.9334608
Co	12.5	0.719	94.248	Co	12.5	0.496	96.032
Cu	103.0	6.286	93.8970874	Cu	103.0	3.554	96.5495146
Fe	8160.0	88.359	98.9171691	Fe	8160.0	68.081	99.165674
Pb	5840.0	0.534	99.9908562	Pb	5840.0	1.082	99.9814726
Mn	167.0	4.902	97.0646707	Mn	167.0	5.674	96.6023952
Ni	430.0	3.816	99.1125581	Ni	430.0	2.652	99.3832558
Se	609.0	0.701	99.8848933	Se	609.0	0.61	99.8998358
Li	6.8	0.0	100.0	Li	6.8	0.0	100.0
V	17.0	0.986	94.2	V	17.0	1.097	93.5470588
Zn	696.0	10.737	98.4573276	Zn	696.0	40.36	94.2011494

3.9 Conclusion

Polymers (NCC-PBG-A and NCC-PBG-B) were made from cellulose extracted from solid waste of the olive industry (OISW) by a process developed at our laboratories. The extracted cellulose was oxidized, and then reacted with phenylbiguanide to prepare the first polymer (NCC-PBG-A) which carries imine and amine groups. The imine groups were then reduced with a borohydride (BH_4^-) to prepare a second polymer (NCC-PBG-B) loaded with amine functional groups. Optimum adsorption conditions such as time, temperature, adsorption dosage, and pH values have been determined to achieve the highest adsorption efficiency for the polymers.

In general, the adsorption rates were high and excellent, in addition to being close in magnitude under most conditions. When studying the contact time, the optimum time for the adsorption of Copper ions Cu^{2+} by both polymers was 10 minutes, the optimal pH value was equal to 7 at room temperature and the optimal adsorbent dosage equal 10.0 mg was optimum for Cu^{2+} adsorption by both polymers. Both polymers showed good adsorption efficiency for copper ions even at small doses of polymers and with relatively high ions concentrations due to the abundance of vacant sites for bonding of metallic ions on the surfaces of the polymers.

The optimum adsorption conditions for the adsorption of Lead ions Pb^{2+} also using the prepared polymers were almost similar to the adsorption conditions for Copper ions Cu^{2+} . A sample was collected from wastewater and treated with the prepared polymers. The removal efficiency of toxic metal ions present in the wastewater sample was high and remarkable.

Recommendations

- a. These polymers can be screened in water treatment for organic pollutants.
- b. The preparation of cellulose polymers can be studied using other materials or other cross-linking agents.
- c. These polymers can be investigated in various applications in different areas of drug administration and the pharmaceutical industry.

References

- [1] Arie H. Havelaar, Augustinus E.M. De Hollander, Peter F.M. Teunis, Eric G. Evers, Henk J. Van Kranen, Johanna, "*Balancing the risks and benefits of drinking water disinfection: disability adjusted life-years on the scale.*," **Environ Health Perspect**, vol. 108, pp. 315–321, February 2000.
- [2] Maryam B. and Büyükgüngör H., "*Wastewater reclamation and reuse trends in Turkey: Opportunities and challenges*," **Journal of Water Process Engineering**, vol. 30, p. 100501, 2019.
- [3] Pandey N., Shukla S. K., and Singh N. B., "*Water purification by polymer nanocomposites: an overview*," **Nanocomposites**, vol. 3, no. 2, pp. 47–66, 2017.
- [4] Rashmi Verma and Pratima Dwivedi, "*Heavy metal water pollution- A case study*," **Science and Technology**, 5(5), pp. 98–99, 2013.
- [5] Mubarak N. M., Sahu J. N., Abdullah E. C., "*Removal of Heavy Metals from Wastewater Using Carbon Nanotubes*," **Separation & Purification Reviews**, vol. 43, no. 4, pp. 311–338, 2014.
- [6] Ramachandra T. V., Ahalya N & Kanamadi R. D., "*Biosorption: Techniques and Mechanisms*," **CES Technical Report 110**, January 2005.
- [7] Bradl H. B., "*Heavy Metals in the Environment_ Origin, Interaction and Remediation-Elsevier* ", Academic Press 2005.
- [8] Jeanne M. Deely, Jack E. Fergusson, "*Heavy metal and organic matter concentrations and distributions in dated sediments of a small estuary*

- adjacent to a small urban area,*” **The Science of the Total Environment**, vol. 153, pp. 97–111, 1994.
- [9] Dai C., Liu Q., Li D., “***Molecular Insights of Copper Sulfate Exposure-Induced Nephrotoxicity: Involvement of Oxidative and Endoplasmic Reticulum Stress Pathways,***” **Biomolecules**, vol. 10, no. 7, 2020.
- [10] Zhang X., Smith R. T., Le C., “***Copper-mediated synthesis of drug-like bicyclopentanes,***” **Nature**, vol. 580, no. 7802, pp. 220–226, 2020.
- [11] Hsiao C. Y., Gresham C., and Marshall M. R., “***Treatment of lead and arsenic poisoning in anuric patients - a case report and narrative review of the literature,***” **BMC nephrology**, vol. 20, no. 1, p. 374, 2019.
- [12] Rifaqat Ali Khan Rao, Moonis Ali Khan, and and Fouzia Rehman, “**Batch and Column Studies for the Removal of Lead(II) Ions from Aqueous Solution onto Lignite,**” January 2011.
- [13] Flora G., Gupta D., and Tiwari A., “***Toxicity of lead: A review with recent updates,***” **Interdisciplinary toxicology**, vol. 5, no. 2, pp. 47–58, 2012.
- [14] Kabeer A., Muhammad Mailafiya M., Danmaigoro A., “***Therapeutic potential of curcumin against lead-induced toxicity: A review,***” **Biomedical Research and Therapy**, vol. 6, no. 3, pp. 3053–3066, 2019.
- [15] Divya Singh, Archana Tiwari and Richa Gupta, “***Phytoremediation of lead from wastewater using aquatic plants,***” **Journal of Agricultural Technology**, 8(1), 2012.
- [16] Teoh Y. P., Khan M. A., and Choong T. S., “***Kinetic and isotherm studies for lead adsorption from aqueous phase on carbon coated***

- monolith*,” **Chemical Engineering Journal**, vol. 217, pp. 248–255, 2013.
- [17] Akinbayo Akinbiyi, Regina, Saskatchewan, **“REMOVAL OF LEAD FROM AQUEOUS SOLUTIONS BY ADSORPTION USING PEAT MOSS,”** November, 2000.
- [18] Jalees M. I., **“Synthesis and application of magnetized nanoparticles to remove lead from drinking water: Taguchi design of experiment,”** **Journal of Water, Sanitation and Hygiene for Development**, vol. 10, no. 1, pp. 56–65, 2020.
- [19] Fakhre N. A. and Ibrahim B. M., **“The use of new chemically modified cellulose for heavy metal ion adsorption,”** **Journal of Hazardous Materials**, vol. 343, pp. 324–331, 2018.
- [20] Alaei Shahmirzadi M. A., Hosseini S. S., Luo J., **“Significance, evolution and recent advances in adsorption technology, materials and processes for desalination, water softening and salt removal,”** **Journal of environmental management**, vol. 215, pp. 324–344, 2018.
- [21] Kyzas G. and Matis K., **“Flotation in Water and Wastewater Treatment,”** **Processes**, vol. 6, no. 8, p. 116, 2018.
- [22] Amal Juma Habish, **“Influence of synthesis parameters on the properties of the composite adsorbents based on sepiolite and nano-zerovalent iron,”** 2017.
- [23] **Kammerer J., Carle R., and Kammerer D. R., “Adsorption and Ion Exchange: Basic Principles and Their Application in Food**

- Processing*,” **Journal of Agricultural and Food Chemistry**, vol. 59, no. 1, pp. 22–42, 2011.
- [24] Kumari P., Alam M., and Siddiqi W. A., “*Usage of nanoparticles as adsorbents for waste water treatment: An emerging trend*,” **Sustainable Materials and Technologies**, vol. 22, e00128, 2019.
- [25] Kavithayeni V., Dr Geetha K., Akash Prabhu S., “*A Review on Dye Reduction Mechanism using Nano Adsorbents in Waste Water*,” **International Journal of Recent Technology and Engineering (IJRTE)**, vol. 7, 6S2, April 2019.
- [26] Henriksson M. and Berglund L. A., “*Structure and properties of cellulose nanocomposite films containing melamine formaldehyde*,” **Journal of Applied Polymer Science**, vol. 106, no. 4, pp. 2817–2824, 2007.
- [27] Bethke K., Palantöken S., Andrei V., “*Functionalized Cellulose for Water Purification, Antimicrobial Applications, and Sensors*,” **Advanced Functional Materials**, vol. 28, no. 23, p. 1800409, 2018.
- [28] Weijun Yang, Guochuang Qi, José Maria Kenny, Debora Puglia, Piming Ma, “*Effect of Cellulose Nanocrystals and Lignin Nanoparticles on Mechanical, Antioxidant and Water Vapour Barrier Properties of Glutaraldehyde Crosslinked PVA Films*” **Polymers**, 12(6), 1364, 2020.
- [29] Kirui A., Ling Z., Kang X., “*Atomic Resolution of Cotton Cellulose Structure Enabled by Dynamic Nuclear Polarization Solid-State*

- NMR*,” **Cellulose (London, England)**, vol. 26, no. 1, pp. 329–339, 2019.
- [30] Carpenter A. W., De Lannoy C. F., and Wiesner M. R., “*Cellulose nanomaterials in water treatment technologies*,” **Environmental science & technology**, vol. 49, no. 9, pp. 5277–5287, 2015.
- [31] Jiahao Jiang, Xiwen Wang, “*Adsorption of Hg(II) Ions from Aqueous Solution by Thiosemicarbazide-modified Cellulose Adsorbent*” **Journal Home Page**, Vol 14, No 2 (2019).
- [32] Kaboorani A. and Riedl B., “*Nano-aluminum oxide as a reinforcing material for thermoplastic adhesives*,” **Journal of Industrial and Engineering Chemistry**, vol. 18, no. 3, pp. 1076–1081, 2012.
- [33] Kaboorani A., Riedl B., Blanchet, “*Nanocrystalline cellulose (NCC): A renewable nano-material for polyvinyl acetate (PVA) adhesive*,” **European Polymer Journal**, vol. 48, no. 11, pp. 1829–1837, 2012.
- [34] Ilyas R. A., Sapuan S. M, and Ishak M. R., “*Isolation and characterization of nanocrystalline cellulose from sugar palm fibres (Arenga Pinnata)*,” **Carbohydrate polymers**, vol. 181, pp. 1038–1051, 2018.
- [35] Bondeson D., Mathew A., and Oksman K., “*Optimization of the isolation of nanocrystals from microcrystalline cellulose by acid hydrolysis*,” **Cellulose**, vol. 13, no. 2, pp. 171–180, 2006.
- [36] Higgins G. A., Joharchi N., and Sellers E. M., “*Behavioral effects of the 5-hydroxytryptamine3 receptor agonists 1-phenylbiguanide and*

- m-chlorophenylbiguanide in rats*,” **The Journal of pharmacology and experimental therapeutics**, vol. 264, no. 3, pp. 1440–1449, 1993.
- [37] Ireland S. J. and Tyers M. B., “*Pharmacological characterization of 5-hydroxytryptamine-induced depolarization of the rat isolated vagus nerve*,” **British Journal of Pharmacology**, vol. 90, no. 1, pp. 229–238, 1987.
- [38] Hamed O., Jodeh S., Al-Hajj N., Abo-Obeid A., Hamed E.M., Fouad Y., “*Cellulose acetate from biomass waste of olive industry*,” **Journal of Wood Science**, 61(1), pp. 45–52, 2015.
- [39] Martinez-Garcia G., Bachmann R., Williams C., Burgoyne A. and Edyvean R., “*Olive oil waste as a biosorbent for heavy metals*,” **Int BiodeterBiodegrad**, 58(3-4), pp. 231–238, 2006.
- [40] Hatakeyama H. T., “*Lignin, Proteins, Bioactive Nanocomposites*,” **Adv. Polym., Sci.** 232, p. 1, 2010.
- [41] Pandey K. C., “*Lignin depolymerization and conversion: a review of thermochemical methods: Pandey MP, Kim CS.*,” **Chem Eng Technol**, vol. 34, pp. 29–41, 2011.
- [42] Coskun T., Debik E. and Demir NM., “*Treatment of Olive Mill Wastewaters by Nanofiltration and Reverse Osmosis Membranes*,” **Elsevier**, pp. 65–70, 2010.
- [43] Ugurlu I. K. M., “*Decolourization and removal of some organic compounds from olive mill wastewater (OMW) by advanced oxidation processes (AOPS) and lime treatment*,” **Environ, Sci. Pollut. Res.** 14, pp. 319–325, 2007.

- [44] Mekki A., Dhouib A., Aloui F. and Sayadi S., ***“Olive wastewater as an ecological fertiliser,” Agron Sustain, Dev 26, pp. 61–67, 2006.***
- [45] Howard R., Abotsi E., Van Rensburg EJ., Howard S., ***“Lignocellulose biotechnology: issues of bioconversion and enzyme production,” Afr J Biotechnol, 2:60, pp. 2–19, 2003.***
- [46] Stenius P., ***“Forest Products Chemistry: Forest Products Chemistry. Papermaking Science and Technology. Fapet Oy: Helsinki,” Papermaking Science and Technology, Fapet Oy: Helsinki, 2000.***
- [47] Essington ML., ***“Soil and Water Chemistry,” An Integrative Approach, 2003.***
- [48] Dargo H., Gabbiye N., Ayalew A., ***“Removal of Methylene Blue Dye from Textile Wastewater using Activated Carbon Prepared from Rice Husk,” International Journal of Innovation and Scientific Research, Vol. 9 (2), pp. 317–325, Sep. 2014.***
- [49] Tan I., Hameed B., Ahmad A., ***“Equilibrium and Kinetic studies on basic dye adsorption by oil palm fiber activated carbon” J. Chem. Eng. 127, pp. 111-119, 2007.***

جامعة النجاح الوطنية

كلية الدراسات العليا

تعديل بلورات السليولوز النانوية بواسطة الأمين العطري : تحضيره وتقييمه كمادة مذيبة لأيونات المعادن السامة

إعداد

مجدي نضال محمد قيسي

بإشراف

أ.د. عثمان حامد

د. إبراهيم أبو شقير

قُدمت هذه الأطروحة استكمالاً لمتطلبات الحصول على درجة الماجستير في الكيمياء بكلية الدراسات العليا في جامعة النجاح الوطنية، نابلس - فلسطين

2021

ب

تعديل بلورات السليولوز النانوية بواسطة الأمين العطري : تحضيره وتقييمه كمادة

مزيلة لأيونات المعادن السامة

إعداد

مجدي نضال محمد قيسي

بإشراف

أ.د. عثمان حامد

د. إبراهيم أبو شقير

الملخص

في الآونة الأخيرة ، تحظى المياه الملوثة بالعناصر السامة الثقيلة باهتمام كبير من العلماء في جميع أنحاء العالم. تميل العديد من الدراسات الحديثة إلى تطوير طرق مناسبة لإزالة هذه المواد السامة من المياه الملوثة ، ومن المهم أن تكون هذه الطرق منخفضة التكلفة وصديقة للبيئة ، بحيث تكون أكثر جاذبية من الناحية التجارية والعملية. في هذه الدراسة ، تم استغلال مزايا السليولوز وتسخيرها في تنقية المياه العادمة الملوثة بأيونات المعادن الثقيلة السامة ، حيث تم تحضير بوليمر ثلاثي الأبعاد متفرع ومتقاطع لاستخدامه في عملية التنقية.

في البداية ، تم تحويل بوليمر السليولوز الطبيعي المستخرج من المخلفات الصلبة لصناعة الزيتون (OISW) إلى السليولوز النانوي البلوري (NCC) ، ثم تم إجراء أكسدة السليولوز النانوي البلوري باستخدام بيرويدات الصوديوم (NaIO_4) لإنتاج ديالديهايد. أخيرًا ، تم تحويل الالديهييد الذي تم الحصول عليه من الخطوة السابقة إلى مجموعات إيمين عن طريق تفاعله مع 1-فينيل بيجوانيد، والذي تم بعد ذلك تحويلها إلى مجموعات أمين باستخدام عامل الاختزال الخفيف بوروهيدريد الصوديوم.

تم تحضير نوعين من البوليمرات: النوع الأول تم تكوينه عند ربط جزيئات 1-فينيل بيجوانيد بمجموعات الألدهيد في السليولوز المؤكسد المحضر في الخطوة السابقة لتشكيل بوليمر السليولوز المعدل (NCC-PBG-A) الذي يحمل مجموعة وظيفية إيمينية ويحمل أيضًا مجموعات وظيفية

أمين. تمت معالجة جزء من البوليمر الذي يحتوي على مجموعة إيمين المنتجة في الخطوة النهائية باستخدام بوروهيدريد الصوديوم لتحضير البوليمر من النوع الثاني (NCC-PBG-B).

تم تحليل البوليمرات المعدة بواسطة FT-IR. تم فحص نشاط البوليمرات وقدرتها على امتصاص أيونات النحاس (Cu^{2+}) والرصاص (Pb^{2+}). تم فحص العوامل التي تؤثر على عملية الامتزاز مثل كتلة المواد الماصة وتركيز أيونات المعادن في المحلول المائي ودرجة الحرارة ودرجة الحموضة والوقت. تم الحصول على أعلى كفاءة للبوليمر (NCC-PBG-A) في إزالة أيونات النحاس (Cu^{2+}) بتركيز 1.0 جزء في المليون، 100.0 مجم من البوليمر، في درجة حرارة الغرفة 25°س، ودرجة الحموضة 7.0 عند التحريك لمدة 10.0 دقائق. أظهر البوليمر نفسه أيضًا كفاءة امتصاص أفضل لأيونات الرصاص (Pb^{2+}) عند تركيز 5.0 جزء في المليون من أيونات الرصاص، 100.0 مجم من البوليمر، في درجة حرارة الغرفة 25°س، ودرجة الحموضة 7.0 عند التحريك لمدة 10.0 دقائق. بالنسبة إلى بوليمر (NCC-PBG-B) ظهرت أعلى كفاءة تجاه أيونات النحاس (Cu^{2+}) عند تركيز 10.0 جزء في المليون من أيونات الرصاص (Pb^{2+})، 50.0 مجم من البوليمر، في درجة حرارة 15.0°س، ودرجة الحموضة 7.0 عند التحريك لمدة 5.0 د. أظهر البوليمر نفسه أيضًا كفاءة امتصاص أفضل لأيونات الرصاص (Pb^{2+}) عند تركيز 15.0 جزء في المليون من أيونات الرصاص، 50.0 مجم من البوليمر، عند درجة حرارة 15.0°س، ودرجة الحموضة 7.0 عند التحريك لمدة 10.0 دقائق.

أظهرت الديناميكا الحرارية والدراسات الحركية أن إزالة أيونات النحاس (Cu^{2+}) والرصاص (Pb^{2+}) باستخدام هذه البوليمرات تتبع حركية الدرجة الثانية. القيمة النظرية لـ q_e (الحسابية) قريبة من حيث القيمة من q_e التجريبية (العملية). يشير هذا إلى أن الامتزاز القوي قد يكون هو المعدل الذي يحدد ظروف عملية الامتزاز. تم تصنيف عملية الامتزاز على أنها طاردة للحرارة، وتوضح

هذه النتائج أنه يمكن توفير هذا العمل بسهولة لصنع مادة ماصة عالية الفعالية.